

Demonstrations, CoT, and Prompting: A Theoretical Analysis of ICL

Xuhan Tong*

Yuchen Zeng^{†1}

Jiawei Zhang^{†2}

Abstract

In-Context Learning (ICL) enables pretrained LLMs to adapt to downstream tasks by conditioning on a small set of input-output demonstrations, without any parameter updates. Although there have been many theoretical efforts to explain how ICL works, most either rely on strong architectural or data assumptions, or fail to capture the impact of key practical factors such as demonstration selection, Chain-of-Thought (CoT) prompting, the number of demonstrations, and prompt templates. We address this gap by establishing a theoretical analysis of ICL under mild assumptions that links these design choices to generalization behavior. We derive an upper bound on the ICL test loss, showing that performance is governed by (i) the quality of selected demonstrations, quantified by Lipschitz constants of the ICL loss along paths connecting test prompts to pretraining samples, (ii) an intrinsic ICL capability of the pretrained model, and (iii) the degree of distribution shift. Within the same framework, we analyze CoT prompting as inducing a task decomposition and show that it is beneficial when demonstrations are well chosen at each substep and the resulting subtasks are easier to learn. Finally, we characterize how ICL performance sensitivity to prompt templates varies with the number of demonstrations. Together, our study shows that pretraining equips the model with the ability to generalize beyond observed tasks, while CoT enables the model to compose simpler subtasks into more complex ones, and demonstrations and instructions enable it to retrieve similar or complex tasks, including those that can be composed into more complex ones, jointly supporting generalization to unseen tasks. All theoretical insights are corroborated by experiments.

1 Introduction

In-Context Learning (ICL) (Brown et al., 2020) is a widely used techniques that enables Large Language Models (LLMs) to perform target tasks by presenting multiple of input-output example pairs, termed *demonstrations*, drawn from the target tasks within the prompt. Since its introduction, ICL has demonstrated strong empirical performance across a broad range of real-world tasks (Agarwal et al., 2024; OpenAI, 2023), including coding (Chen, 2021), math problem solving (Hendrycks et al., 2021b; Cobbe et al., 2021) and question answering (Rein et al., 2024; Hendrycks et al., 2021a). Despite these empirical successes, the theoretical understanding of ICL remains limited, as existing analyses suffer from at least one of the two limitations described below.

First, many theoretical studies rely on strong simplifying assumptions, including linear attention (Ahn et al., 2023; von Oswald et al., 2023; Mahankali et al., 2024; Zhang et al., 2024; Cui et al., 2025), single-layer transformers or attention-only architectures (Yang et al., 2024b; von Oswald

* Department of Computer Sciences, University of Wisconsin-Madison. tong56@wisc.edu.

[†] Co-last authors. ¹ Microsoft Research. yuchen.zeng.1998@gmail.com. ² Department of Computer Sciences, University of Wisconsin-Madison. jzhang2924@wisc.edu.

Our code is available at: <https://github.com/txxxxh/Demonstrations-CoT-and-Prompting>.

et al., 2023; Akyürek et al., 2023; Dai et al., 2023; Mahankali et al., 2024; Zhang et al., 2024; Cui et al., 2025), single-head attention (Yang et al., 2024a; Zhang et al., 2023), or random generalized linear regression data distributions (Ahn et al., 2023; von Oswald et al., 2023; Oko et al., 2024; Zhang et al., 2024; Fu et al., 2024). While these assumptions enable tractable analysis, they abstract away architectural and data properties that are critical in practice.

Meanwhile, intuitively, by observing demonstrations, the model can better infer the underlying task intent that defines desirable outputs. Extensive empirical studies have therefore focused on how to construct effective demonstrations, showing that factors such as the number of demonstrations (Agarwal et al., 2024), their selection (Liu et al., 2022; Su et al., 2023), prompt template (Ye et al., 2024), and the inclusion of Chain-of-Thought (CoT (Wei et al., 2022)) reasoning in demonstrations can lead to substantial differences in performance. However, most theoretical work fail to depict how these key practical factors affect ICL performance (Feng et al., 2023; Li et al., 2023; Tutunov et al., 2024). To bridge this gap, in this paper, we present a set of theoretical results under mild assumptions, all of which are corroborated by corresponding synthetic experiments.

Our Contributions. Under the above formulation, we provide a theoretical characterization of how demonstration selection, CoT, prompt template, number of demonstrations influences ICL performances. Our main contributions are summarized as follows.

- **Quantifying Demonstration Effectiveness via Lipschitz Constants.** We prove that when ICL is used to adapt a pretrained model to a downstream task with an unseen test prompt, the performance is governed by three factors. The first is the effectiveness of the demonstration in identifying the target task, captured by the minimum Lipschitz constant of the ICL loss along a path that maps the test prompt to any sample observed during pretraining. A large Lipschitz constant indicates that the demonstrations fail to stably pin down the underlying task. In addition, the analysis also captures the effects of the pretrained model’s intrinsic ICL capability and the distance between the test prompt and pretraining prompts, which reflects the degree of distribution shift.
- **Characterizing When CoT Benefits ICL.** We next consider the setting where demonstrations include CoT traces, which can be viewed as decomposing the target task into multiple subtasks. We show that the loss on the test prompt can be decomposed into a weighted sum of the losses incurred when performing ICL on these subtasks, where the weights are determined by the Lipschitz constants of the loss along paths that map subtask-specific samples in the test prompt to the corresponding subtask samples in the pretraining dataset. This result indicates that CoT is beneficial to ICL when the task decomposition selects well-learned subproblems and when the demonstrations for each subtask are chosen such that the subtasks are well-defined and reliably identifiable.
- **Establishing the Interaction Between Prompt Templates and Demonstration Count.** We show that the influence of prompt templates on ICL exhibits a mixed effect that depends on the number of demonstrations. By analyzing changes in output logits with respect to the prompt template, we prove that this influence is generally upper bounded by an exponential decay in the number of demonstrations. Consequently, when the number of demonstrations is small, prompt templates can substantially affect output probabilities, whereas as the number of demonstrations increases, ICL performance becomes increasingly invariant to the choice of prompt template. An important exception arises when prompt templates provide different incorrect instructions across demonstrations, in which case this decay no longer holds.

All of our theoretical results are supported by experiments.

Our results can be understood through the model’s ability to generalize beyond pretraining. First, we show that pretraining enables the model to generalize to tasks that are similar to those seen during training. Building on this, demonstrations in a prompt enable the model to retrieve such tasks during ICL: given sufficiently informative examples, the model can map the test prompt to tasks that were either seen during pretraining, similar to them, or composed from them, with the retrieval becoming more reliable as the number of demonstrations increases. Furthermore, CoT extends this capability by enabling generalization to more complex tasks: if a task can be decomposed into subtasks that are well learned during pretraining, then the model can combine them to solve the overall task. Together, these results show that ICL leverages pretraining to generalize not only to similar tasks, but also to their compositions, with demonstrations and CoT serving as mechanisms for retrieving and composing such knowledge.

2 Lipschitz Characterization of Demonstration Effectiveness in ICL

2.1 Background

We start by presenting our problem setting for analyzing ICL with a test prompt unseen through pretraining. Let \mathcal{V} denote a finite vocabulary, and let \mathcal{V}^L denote the set of all symbol sequences of length at most L . Since \mathcal{V} is finite and the sequence length is bounded, \mathcal{V}^L is a finite (and hence compact) set. We write $\mathcal{V}^* := \mathcal{V}^L$. A data sample is denoted by (x, y) , where $x, y \in \mathcal{V}^*$. Let \mathcal{M} denote a class of Transformer models, where each $M \in \mathcal{M}$ is a function $M : \mathcal{V}^* \rightarrow \mathcal{V}^*$ that maps an input prompt sequence to its continuation. We assume the existence of a target model $M_\star : \mathcal{V}^* \rightarrow \mathcal{V}^*$ that is optimized for performing ICL on a given target task. Such a target model is commonly assumed in theoretical analyses (Zeng and Lee, 2024; Giannou et al., 2023). This assumption is realistic because the Transformer class is a universal sequence-to-sequence approximator (Yun et al., 2020) and can represent a broad range of target tasks. Moreover, introducing M_\star lets us carry out the analysis within a well-defined hypothesis space \mathcal{M} , rather than imposing additional structural assumptions on the target task.

We consider a pretrained Transformer model $M \in \mathcal{M}$, and denote the test prompt as $\mathbf{z} = (x_1, y_1, \dots, x_n, y_n, x_{\text{query}})$, where $n \in \mathbb{N}$ is the number of demonstrations and $x_{\text{query}} \in \mathcal{V}^*$ is the query. The *ICL loss* is defined as $\ell_{\text{ICL}}(\mathbf{z}) := |M(\mathbf{z}) - M_\star(\mathbf{z})|$. Finally, let domain $D_0 \subset \mathcal{V}^*$ denote the set of pretraining prompts that contain a variable number of demonstrations.

To establish our main results, we will rely on two classical tools from approximation theory, which we recall below.

Lemma 2.1 (Remez Inequality for Polynomials (Remez, 1936)). *If $J \in \mathbb{R}$ is a finite interval, and $E \subset J$ is an arbitrary measurable set, then for any polynomial p of degree n ,*

$$\max_{x \in J} |p(x)| \leq \left(\frac{4 \text{mes}(J)}{\text{mes}(E)} \right)^n \sup_{x \in E} |p(x)|.$$

Lemma 2.2 (Bernstein Approximation Theorem, Lipschitz Case (Lorentz, 1986)). *Let $f : [0, 1] \rightarrow \mathbb{R}$ be a Lipschitz continuous function with Lipschitz constant L . Let $B_n f$ denote the degree- n Bernstein polynomial (see Appendix C for definition) approximation of f . Then, for all $n \geq 1$,*

$$\sup_{x \in [0, 1]} |B_n f(x) - f(x)| \leq \frac{L}{2\sqrt{n}}.$$

2.2 Lipschitz Generalization Bound

We now combine the above ingredients to characterize how effectively in-context demonstrations identify the target task and control generalization to unseen prompts.

Theorem 2.3 ((Informal) ICL Generalization Bound). *For any test prompt $\mathbf{z} \in D \setminus D_0$ that is unseen during pretraining, the ICL loss satisfies*

$$\ell_{ICL}(\mathbf{z}) \leq O(\kappa^{L^2}) \sup_{\mathbf{z}' \in D_0} \ell_{ICL}(\mathbf{z}'),$$

where L is an effective Lipschitz parameter determined by the smallest Lipschitz constant of ℓ_{ICL} along straight-line paths connecting the test prompt \mathbf{z} to pretraining prompts $\mathbf{z}' \in D_0$, and $\kappa > 1$ quantifies the degree of distribution shift.

Proof Sketch. The key idea of this proof is to use Remez-Chebyshev inequality (Lemma 2.1). The main difficulty is that the loss $\ell_{ICL}(\cdot)$ is *not* a polynomial and is defined over the prompt space rather than a one-dimensional interval. Here we introduce two reductions before applying Lemma 2.1.

1. *Step 1: Reduce the prompt space to a finite interval via a path.* Fix an unseen test prompt $\mathbf{z} \notin D_0$ and pick any $\mathbf{z}' \in D_0$. Consider the straight-line path $\gamma : [0, 1] \rightarrow \mathcal{V}^*$,

$$\gamma(t) = \mathbf{z}' + t(\mathbf{z} - \mathbf{z}'),$$

so that $\gamma(0) = \mathbf{z}'$ and $\gamma(1) = \mathbf{z}$. Restricting the loss to this path yields a function on a compact interval,

$$\ell'_{ICL}(t) \triangleq \ell_{ICL}(\gamma(t)), \quad t \in [0, 1].$$

This step converts the domain requirement of Remez–Chebyshev (a finite interval) into our setting.

2. *Step 2: Convert a Lipschitz function into a polynomial via Bernstein approximation.* Remez–Chebyshev applies to polynomials, so we approximate the (generally non-polynomial) function ℓ'_{ICL} by a degree- n Bernstein polynomial $B_n \ell'_{ICL}$. Since ℓ'_{ICL} is Lipschitz on $[0, 1]$ with constant denoted by L_γ , applying Lemma 2.2 gives

$$\sup_{t \in [0, 1]} |B_n \ell'_{ICL}(t) - \ell'_{ICL}(t)| \leq \frac{L_\gamma}{2\sqrt{n}}. \quad (1)$$

This is the key trick that allows us to manufacture a polynomial while controlling the approximation error explicitly.

3. *Step 3: Apply Remez-Chebyshev to the polynomial surrogate.* We now apply Lemma 2.1 to the polynomial $B_n \ell'_{ICL}$ on the interval $[0, 1]$, with any subset $E \subset [0, 1]$ satisfying

$$E \supset \{t \in [0, 1] : \gamma(t) \in D_0\},$$

and has positive measure. This yields

$$\max_{t \in [0, 1]} |B_n \ell'_{ICL}(t)| \leq C_\gamma^n \sup_{t \in E} |B_n \ell'_{ICL}(t)| \quad (2)$$

for a universal constant $C_\gamma > 1$ (equivalently, $C_\gamma = 4 \text{mes}([0, 1]) / \text{mes}(E)$ in the statement of Lemma 2.1).

4. *Step 4: Transfer the bound back to ℓ_{ICL} and choose n .* Combining the Equation (1) and Equation (2) yields

$$\max_{t \in [0,1]} \ell'_{ICL}(t) \leq C_\gamma^n \sup_{t \in E} \ell'_{ICL}(t) + O\left(\frac{L_\gamma}{\sqrt{n}}\right).$$

Finally, evaluating at $t = 1$ gives the desired bound for $\ell_{ICL}(\mathbf{z}) = \ell'_{ICL}(1)$, and taking a optimal γ by selecting over $\mathbf{z}' \in D_0$ completes the proof. Complete details are provided in Appendix C. \square

Remark 2.4. Our analysis connects a test query $\mathbf{z} \in D$ to a pretraining prompt $\mathbf{z}' \in D_0$, which implicitly assumes compatible sequence lengths. In practice, pretraining sequences are often longer than ICL queries. We therefore allow \mathbf{z} to be extended by *virtual padding* (also used in Theorem 3.1 and Section 4.1); a formal justification is given in Appendix D.2. Moreover, our setup focuses on greedy decoding (temperature = 0), where the model output is a single token. More general settings that account for distributional outputs are deferred to Section 4.

Theorem 2.3 suggests that ICL performance on an unseen prompt is governed by three factors: (i) the model’s intrinsic ICL capability, captured by $\sup_{\mathbf{z}' \in D_0} |\ell_{ICL}(\mathbf{z}')|$; (ii) an effective Lipschitz parameter L that quantifies how stably the demonstrations identify the underlying task; and (iii) prompt distribution, characterized by κ . expansion. The first factor is straightforward: even if the demonstrations perfectly specify the task, a model with weak intrinsic ICL ability (interpreted as *large pretraining error*) may still incur large loss. The second factor is more subtle and reflects *task ambiguity* induced by the demonstrations. The third factor captures how far the test prompt deviates from pretraining prompts.

Intuitively, L measures how rapidly the loss can change as we move from the test prompt toward the pretraining prompts. When the demonstrations do not uniquely pin down a task, small perturbations of the prompt can switch the most plausible task interpretation, which in turn can lead to a large change in the model’s predicted output distribution and the resulting loss. In this regime, the loss landscape is “steep” along prompt-space paths, corresponding to a large effective Lipschitz parameter.

A concrete example illustrates this phenomenon. Consider the prompt

Japan \rightarrow Tokyo, France \rightarrow Paris, USA \rightarrow ?

This context is compatible with multiple latent task hypotheses, such as mapping countries to their capitals or mapping countries to their largest cities. Under different hypotheses, the appropriate continuation could be either **Washington DC** or **New York**. As a result, small perturbations of the prompt—such as modifying or replacing a single demonstration—can shift which hypothesis best explains the context, leading to a large change in the model’s continuation distribution for **USA** \rightarrow . This behavior corresponds to a large effective Lipschitz L : the loss can vary sharply because the demonstrations fail to robustly resolve task ambiguity.

In contrast, consider the prompt

Australia \rightarrow Sydney, Turkey \rightarrow Istanbul, USA \rightarrow ?

In this case, the demonstrations more strongly favor a single underlying task interpretation, such as mapping countries to their largest cities, while disfavoring alternative hypotheses (e.g., mapping to capitals). As a result, the task identity is more clearly specified, and small variations of the prompt are unlikely to change the inferred task.

This corresponds to a smaller effective Lipschitz L , indicating that the demonstrations provide a more stable alignment between the unseen prompt and a coherent task seen during pretraining.

Remark 2.5. This result shows that pretraining equips the model with an intrinsic ability to generalize from observed tasks to related tasks, thereby inducing a structured task space beyond those explicitly seen during training.

In Section 3, we will show how this Lipschitz parameter governs when CoT can improve ICL. In Section 4, we will further show that Lipschitz continuity characterizes the magnitude of variation between different prompt templates. A small Lipschitz guarantees uniformly small variation of function value along the path, and hence strong generalization. This distinction explains why certain CoT constructions or prompt formats may succeed or fail to generalize reliably across prompts.

3 CoT in ICL: A Lipschitz-Based Perspective

3.1 Problem Setup

Chain-of-thought (CoT) prompting (Wei et al., 2022) is a powerful technique for eliciting multi-step reasoning in large language models by including intermediate reasoning steps in the demonstrations. In this section, we analyze how CoT prompting influences ICL performance. To this end, we extend the notation introduced in Section 2.1 to account for settings in which intermediate steps are explicitly provided.

We assume that the target task can be decomposed into K sequential subtasks. Accordingly, we represent the input as $x = x^{(0)}$, the final output as $y = x^{(K)}$, and the intermediate reasoning steps as $x^{(1)}, \dots, x^{(K-1)}$. Each data sample is thus denoted by the sequence $(x^{(0)}, \dots, x^{(K)})$.

Under this formulation, the test prompt without generating any new intermediate steps is

$$\mathbf{z}^{(0)} = \mathbf{z} = (x_1^{(0)}, \dots, x_1^{(K)}, \dots, x_n^{(0)}, \dots, x_n^{(K)}, x_{\text{query}}^{(0)}),$$

and the prompt augmented with the first $k = 1, \dots, K - 1$ intermediate steps is denoted by

$$\mathbf{z}^{(k)} = (x_1^{(0)}, \dots, x_1^{(K)}, \dots, x_n^{(0)}, \dots, x_n^{(K)}, x_{\text{query}}^{(0)}, \dots, x_{\text{query}}^{(k)}).$$

Accordingly, for each step $k \in 0, \dots, K - 1$, let $D_0^{(k)}$ denote the set of pretraining prompts that contain n demonstrations and k intermediate steps.

3.2 ICL Generalization Bound in the Presence of CoT

Theorem 3.1 ((Informal) ICL Generalization Bound with CoT Prompting). *For a test ICL prompt \mathbf{z} with CoT demonstrations consisting of K steps, the ICL loss satisfies*

$$\ell_{ICL}(\mathbf{z}) \leq \sum_{k=0}^{K-1} O\left(\exp(L_{(k)}^2)\right) \cdot \sup_{\mathbf{z}^{(k)} \in D_0^{(k)}} \ell_{ICL}(\mathbf{z}^{(k)}),$$

where $L_{(k)}$ denotes the effective Lipschitz parameter associated with the k -th subtask.

Theorem 3.1 formalizes the role of CoT in ICL by decomposing its effect into two theoretically grounded components. The bound separates the contribution of the model’s intrinsic ICL capability at each intermediate step, measured by $\sup_{\mathbf{z}^{(k)} \in D_0^{(k)}} \ell_{ICL}(\mathbf{z}^{(k)})$, from the contribution of the effective Lipschitz parameters $L_{(k)}$ induced by the task decomposition. In practice, modern pretrained models often already exhibit strong intrinsic CoT capability, so that $\sup_{\mathbf{z}^{(k)} \in D_0^{(k)}} \ell_{ICL}(\mathbf{z}^{(k)})$ is comparable to the no-CoT case $\sup_{\mathbf{z} \in D_0} \ell_{ICL}(\mathbf{z})$. Under this regime, the theory predicts that the primary benefit

of CoT arises from its ability to reduce the effective Lipschitz parameters of the induced subtasks. As discussed in Section 2.2, these parameters characterize how sensitively the ICL loss varies along prompt-space paths. With CoT, $L_{(k)}$ depends on whether each subtask is well aligned with the pretrained distribution and whether the demonstrations at that step stably identify the subtask. This explains how CoT improves generalization: it succeeds when it reshapes a complex task into subtasks that are both familiar to the model and more specified by the demonstrations. Complete proof is provided in Appendix E.

Remark 3.2. This result further shows that the pretrained model can extend beyond individual tasks to their compositions (see Section 5.2). When a complex task can be decomposed into subtasks that are well learned during pretraining, the model can generalize to such compositional tasks through multi-step reasoning.

4 Synergistic Effects of Demonstration Count and Prompt Templates in ICL

In this section, we study how the number of demonstrations and the choice of prompt templates jointly affect ICL.

4.1 Problem Setup

We consider ICL prompts with varying numbers of demonstrations N and varying prompt templates, where each prompt template is instantiated as an instruction $i \in \mathcal{V}^*$.

Latent Task Model. We assume data are generated from a latent task variable $t \in \mathcal{T}$, where \mathcal{T} is a finite set of tasks. Each task t induces a task-conditional data-generating process. Let $P(\cdot)$ to denote probability distributions and $p(\cdot)$ for the corresponding probability mass or density functions. Conditioned on t , inputs and outputs are generated as

$$x \sim P_{x|t}, \quad y = f_t(x),$$

where $f_t : \mathcal{V}^* \rightarrow \mathcal{V}^*$ is a (possibly unknown) task-specific input-output mapping. We assume a strictly positive prior over tasks,

$$\pi(t) := \mathbb{P}(t = t) > 0 \quad \text{for all } t \in \mathcal{T}.$$

Instructions. A single task may admit multiple valid instructions. We model instructions as random variables drawn from a task-conditional distribution $i \sim P_{i|t}$. For a target task $t^* \in \mathcal{T}$, we say that an instruction i is *correct* for t^* if

$$p(i | t^*) > p(i | t) \quad \text{for all } t \in \mathcal{T} \setminus \{t^*\}.$$

Otherwise, the instruction is said to be *incorrect* for t^* .

Prompt Formats. An ICL prompt consists of demonstrations followed by a query. Depending on how instructions appear in the prompt, we consider the following formats.

1. Single correct instruction (appears once).

$$z = (i, (x_1, y_1), \dots, (x_N, y_N), x_{\text{query}}).$$

Example: *Please add the two numbers.* $1, 2 \rightarrow 3; 4, 5 \rightarrow 9; 6, 7 \rightarrow ?$.

2. Single incorrect instruction (appears once or absent).

$$\mathbf{z} = (\tilde{i}, (x_1, y_1), \dots, (x_N, y_N), x_{\text{query}}),$$

where \tilde{i} is input i or a virtual token $\langle \text{pad} \rangle$.

Example: *Please subtract the two numbers.* $1, 2 \rightarrow 3; 4, 5 \rightarrow 9; 6, 7 \rightarrow ?$.

3. Repeated correct instruction (shared).

$$\mathbf{z} = ((i, x_1, y_1), \dots, (i, x_N, y_N), (i, x_{\text{query}})).$$

Example: $1+2 \rightarrow 3; 4+5 \rightarrow 9; 6+7 \rightarrow ?$.

4. Repeated incorrect instruction (shared).

$$\mathbf{z} = ((i, x_1, y_1), \dots, (i, x_N, y_N), (i, x_{\text{query}})).$$

Example: $1-2 \rightarrow 3; 4-5 \rightarrow 9; 6-7 \rightarrow ?$.

5. Varying correct instructions (one per demonstration).

$$\mathbf{z} = ((i_1, x_1, y_1), \dots, (i_N, x_N, y_N), (i_{\text{query}}, x_{\text{query}})).$$

Example: $1+2 \rightarrow 3; \text{sum}(4, 5) \rightarrow 9; 6 \text{ plus } 7 \rightarrow ?$.

6. Varying incorrect instructions (one per demonstration).

$$\mathbf{z} = ((i_1, x_1, y_1), \dots, (i_N, x_N, y_N), (i_{\text{query}}, x_{\text{query}})).$$

Example: $1-2 \rightarrow 3; \text{product}(4, 5) \rightarrow 9; 6 \bmod 7 \rightarrow ?$.

For notational convenience, we use \mathbf{i} to denote the collection of all instructions appearing in a prompt, regardless of the specific prompt format. Unless otherwise specified, we assume that input-output pairs (x, y) are drawn i.i.d., and that instructions \mathbf{i} are drawn i.i.d. whenever more than one instruction appears in the prompt, independently of the input-output pairs (x, y) .

Pretraining via cross-entropy recovers the Bayesian predictor. Under the latent-task framework introduced above, pretraining can be viewed as learning a conditional predictor $q(\cdot | \mathbf{z})$ by minimizing the empirical cross-entropy loss over a dataset $\{(\mathbf{z}^{(m)}, y^{(m)})\}_{m=1}^M$:

$$q^*(\mathbf{z}) \in \arg \min_{q(\cdot | \mathbf{z})} \frac{1}{M} \sum_{m=1}^M \left[-\log q(y^{(m)} | \mathbf{z}^{(m)}) \right].$$

In the population limit $M \rightarrow \infty$, this objective converges to minimizing the expected log-loss $\mathbb{E}_{(\mathbf{z}, y)} [-\log q(y | \mathbf{z})]$ over all conditional predictors $q(\cdot | \mathbf{z})$. It is well known that the unique minimizer of this objective is the Bayesian posterior-predictive distribution,

$$p(y_{\text{query}} | \mathbf{z}) = \sum_{t \in \mathcal{T}} p(y_{\text{query}} | x_{\text{query}}, t) p(t | \mathbf{z}),$$

which is Bayes-optimal under the log-loss. Accordingly, throughout our analysis we assume that idealized pretraining recovers this Bayesian predictor at the level of conditional distributions, up to standard approximation error.

4.2 When Sensitivity to Prompt Templates Vanishes with Demonstrations

To analyze how the influence of prompt templates evolves as the number of demonstrations increases, we require a mild identifiability condition on the latent tasks. This assumption ensures that different tasks induce distinguishable data-generating distributions, allowing the model to infer the underlying task from sufficiently many demonstrations.

Assumption 4.1 (Identifiability of Tasks). For any two distinct tasks $t_1, t_2 \in \mathcal{T}$ with $t_1 \neq t_2$, the corresponding task-conditional joint distributions are strictly distinguishable, in the sense that $\text{KL}(P_{x,y|t_1} \parallel P_{x,y|t_2}) > 0$.

Assumption 4.2 (Bounded Instruction Sensitivity). There exists a constant $L_i > 0$ such that for all $t \in \mathcal{T}$, $\|\nabla_{\mathbf{i}} \log p(\mathbf{i} | t)\| \leq L_i$.

Based on this assumption, we establish the following result, which shows that the sensitivity of the model output to prompt templates decays exponentially with the number of demonstrations for prompt formats 1-5.

Theorem 4.3 (Exponential Convergence of Posterior Predictive (Formats 1–5)). *Consider prompt formats 1–5. Under Assumptions 4.1 and 4.2, there exist constants $\alpha, \beta > 0$ such that, with high probability, for all sufficiently large numbers of demonstrations N ,*

$$|p(y_{\text{query}} | \mathbf{z}) - p(y_{\text{query}} | x_{\text{query}}, t^*)| \leq \beta \exp(-\alpha N).$$

Equivalently, for any two instructions \mathbf{i}, \mathbf{i}' (with all non-instruction parts of \mathbf{z} fixed), we have

$$|p(y_{\text{query}} | \mathbf{z}(\mathbf{i})) - p(y_{\text{query}} | \mathbf{z}(\mathbf{i}'))| \leq 2\beta \exp(-\alpha N).$$

Corollary 4.4 (Gradient Decay of Prompt Sensitivity). *Under the conditions of Theorem 4.3, then there exist constants $\alpha', \beta' > 0$ such that, with high probability, for all sufficiently large N ,*

$$\|\nabla_{\mathbf{i}} p(y_{\text{query}} | \mathbf{z})\| \leq \beta' \exp(-\alpha' N).$$

Corollary 4.5 (Expected Instruction Stability). *Fix a demonstration count N and consider prompts of formats 1–5 with exactly N demonstrations. Let $q_{\theta}(\mathbf{z}) := p_{\theta}(y_{\text{query}} | \mathbf{z})$ be a predictor learned by cross-entropy training. There exists an $\varepsilon_N \geq 0$ such that, with high probability, for all sufficiently large N and all $\mathbf{i}, \mathbf{i}' \in D$,*

$$\begin{aligned} & \mathbb{E}_{\mathbf{z}} \left[|q_{\theta}(\mathbf{z}(\mathbf{i})) - q_{\theta}(\mathbf{z}(\mathbf{i}'))| \right] \\ & \leq \underbrace{2\beta e^{-\alpha N}}_{\text{demonstrations effect}} + \underbrace{2\mathbb{E}_{\mathbf{z}} \left[|q_{\theta}(\mathbf{z}) - q^*(\mathbf{z})| \right]}_{\text{pretraining effect}}. \end{aligned} \tag{3}$$

Remark 4.6. Equation (3) decomposes instruction sensitivity into task identification from demonstrations and the discrepancy between q_{θ} and $q^*(\mathbf{z})$. The first term captures the effect of demonstrations and decays exponentially with the number of demonstrations N , as established in Theorem 4.3. The second term measures the expected discrepancy between the learned predictor q_{θ} and the Bayesian predictor q^* , reflecting finite pretraining and optimization effects, and is controlled by how well the chosen model class can approximate the Bayesian predictor under the training distribution.

Theorem 4.3 provides a theoretical explanation for a commonly observed empirical phenomenon: the influence of prompt templates tends to diminish as the number of demonstrations increases. In the low-data regime, prompt templates can have a substantial effect on the model’s behavior; however, as more demonstrations are provided, their impact is rapidly suppressed by the evidence contained in the demonstrations themselves.

Importantly, the theorem applies to a broad range of practical prompting scenarios. It covers settings in which the instruction is correct, incorrect (e.g., systematically replacing + with -), or even absent. In all such cases, a sufficient number of demonstrations allows the model to reliably infer the underlying task and produce correct predictions, despite potentially misleading prompt templates. The theorem does not, however, extend to prompt format 6, which represents a fundamentally more challenging regime.

In practice, much of the data we encounter has exactly the structure discussed in this section: an instruction paired with a corresponding input and output. The instruction itself may be different phrasings of the same underlying task. Therefore, training on data with this structure also covers a broad range of scenarios. Complete details are provided in Appendix F.

4.3 When Sensitivity to Prompt Templates Does not Vanishes with Demonstrations

We now turn to prompt format 6, and examine how prompt sensitivity behaves in this case.

Problem setup. We consider \mathbf{i} in a d -dimensional Euclidean instruction space \mathcal{V}^* , whose dimension scales linearly with the number of demonstrations. All gradients and norms with respect to instruction variables are taken with respect to this Euclidean structure.

Here we distinguish two instruction domains. We denote by $D_{\mathbf{i}_0} \subset \mathcal{V}^*$ an *inner instruction domain*, corresponding to the set of instruction variables induced by prompt formats 1-5. We further consider an extended instruction domain $D_{\mathbf{i}} \supset D_{\mathbf{i}_0}$, corresponding to prompt format 6. For analytical convenience, we characterize these domains geometrically by Euclidean balls: there exist radius $0 < r < R < \infty$ such that $B_r \subset D_{\mathbf{i}_0} \subset D_{\mathbf{i}} \subset B_R$, where B_r and B_R denote Euclidean balls in \mathcal{V}^* with radius r and R .

Sensitivity to Prompt Templates. Fix all non-instruction components of the prompt \mathbf{z} , view $f(\mathbf{i}) := p(y_{\text{query}} \mid \mathbf{z})$ as a scalar-valued function defined on \mathcal{V}^* , and let $f^* := p(y_{\text{query}} \mid x_{\text{query}}, t^*)$. We now present our result for prompt format 6.

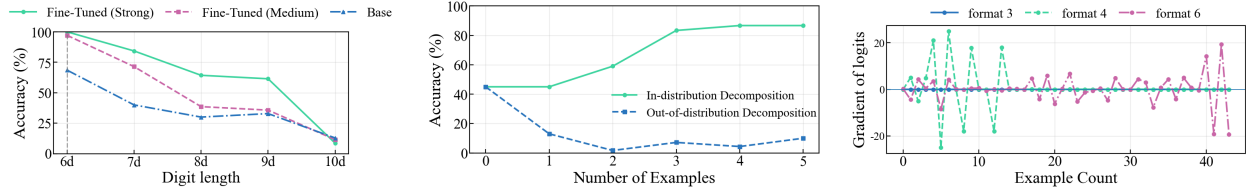
Theorem 4.7 ((Informal) Failure of Convergence of Posterior Predictive (Format 6)). *Consider prompt format 6, under Assumptions 4.1 and 4.2, there exist constants $\alpha, \beta > 0$ and $\epsilon > 0$ such that, with high probability, for all sufficiently large N ,*

$$|f(\mathbf{i}) - f^*| \leq O(\exp(L_{\mathbf{i}}^2))(\beta e^{-\alpha N} + \epsilon).$$

Equivalently, for any two instruction sequences \mathbf{i}, \mathbf{i}' (with all non-instruction parts of \mathbf{z} fixed), we have

$$|f(\mathbf{i}) - f(\mathbf{i}')| \leq 2 \cdot O(\exp(L_{\mathbf{i}}^2))(\beta e^{-\alpha N} + \epsilon).$$

where $L_{\mathbf{i}}$ is the effective instruction-Lipschitz parameter. In particular, the bound does not vanish as $N \rightarrow \infty$ due to the non-decaying term ϵ .



(a) **ICL accuracy on six- to ten-digit addition for three model variants with different intrinsic ICL capability.** Performance follows intrinsic ICL capability near the pretraining distribution, but as input digit length increases and the shift grows, performance gaps shrink and models converge to similarly low accuracy, indicating the Lipschitz constant dominates the performance bound. (b) **Effect of task decomposition quality in CoT prompting.** In-distribution decomposition, where each subtask aligns with computations learned during pretraining, substantially improves performance. In contrast, out-of-distribution decomposition performs worse than vanilla ICL without CoT and degrades further as the number of demonstrations increases. (c) **Average gradient magnitude of output logits with respect to instruction tokens under different prompt formats.** With correct or consistently correct/incorrect instructions (prompts 3 and 5), sensitivity is low or decays as demonstrations increase, whereas with inconsistent incorrect instructions (prompt 6), sensitivity persists and even increases with more demonstrations.

Figure 1: Empirical validation of (a) Theorem 2.3, (b) Theorem 3.1, and (c) Theorems 4.3 and 4.7, respectively.

Corollary 4.8 ((Informal) Failure of Prompt Sensitivity Decay (format 6)). *Under the conditions of Theorem 4.7, there exist constants $\alpha', \beta' > 0$ and $\epsilon' > 0$ such that, with high probability, for all sufficiently large N ,*

$$\sup_{\mathbf{i} \in D_{\mathbf{i}}} \|\nabla_{\mathbf{i}} f(\mathbf{i})\| \leq O(L_{\mathbf{i}}^4 \cdot \exp(L_{\mathbf{i}}^2)) (\beta' e^{-\alpha' N} + \epsilon'),$$

where $L_{\mathbf{i}}$ is the effective Lipschitz parameter implied by Assumption 4.2.

Theorem 4.7 provides a theoretical explanation for the empirical observation that prompt sensitivity may persist even as the number of demonstrations increases, particularly when instructions vary across demonstrations (format 6). In this setting, the model may struggle to reconcile conflicting instructions, leading to poor performance on the target task.

Both Corollary 4.4 and 4.8 concretely instantiate the *Lipschitz intuition* discussed in Section 2.2. In the present setting, the relevant Lipschitz constant corresponds to the effective Lipschitz continuity of $p(y_{\text{query}} | \mathbf{z})$ over domain $D_{\mathbf{i}}$. When the number of demonstrations N is large, Corollary 4.4 shows that the gradient of f goes to zero. This implies a small effective Lipschitz constant along the instruction-induced paths, which (by Theorem 2.3) leads to strong generalization. In contrast, Corollary 4.8 demonstrates that for prompt format 6 the instruction gradient remains large. This corresponds to a large effective Lipschitz constant which prevent meaningful generalization. Complete details are provided in Appendix G.

Remark 4.9. Combining the above results, ICL can be understood as a retrieval process over the pretraining-induced task space. Given demonstrations in the prompt, the model can identify tasks that are (i) seen during pretraining, (ii) similar to them, or (iii) compositions of such subtasks. As the number of demonstrations increases, this retrieval becomes more reliable, enabling the model to select and assemble the appropriate task for the test input.

5 Experiments

5.1 Quantifying Demonstration Effectiveness under Prompt Shift

In Theorem 2.3, we show that ICL performance on unseen prompts is governed by a Lipschitz constant, which depends on the pretrained model’s intrinsic ICL capability and the quality of the selected demonstrations. Accordingly, we design two experiments to validate the effects of these two factors on ICL performance.

Impact of Intrinsic ICL Capability and Prompt Shift. To study how intrinsic ICL capability affects performance, we prepare three variants of Llama3.2-3B with different levels of intrinsic ICL capability. **(Setup)** We consider the number addition task. (i) **Llama3.2-3B-Fine-Tuned (Strong)**: We randomly generate 20,000 six-digit addition sequences and fine-tune the model on them. (ii) **Llama3.2-3B-Fine-Tuned (Medium)**: We concatenate all generated sequences into a single large prompt and fine-tune the model on this single prompt. (iii) **Llama3.2-3B-Base (Weak)**: We use the base model without any additional training. We evaluate them on six- to ten-digit addition to examine how intrinsic ICL capability affects ICL performance on 350 unseen prompts. **(Results)** Test accuracy consistently follows the ordering of intrinsic ICL capability, corroborating our theoretical prediction. Notably, as the inference task moves further away from the pretraining distribution, i.e., with increasing digit length, the performance gap narrows. This is consistent with the regime where the Lipschitz constant dominates the bound: when the task shift is sufficiently large, even strong intrinsic ICL capability cannot prevent degraded ICL performance. See Appendix H.1 for detailed setup.

Impact of Demonstration Choice. We design two tasks for investigating the effect of demonstration choice. **(Task 1. Sport Identification)** Given a country, the task is to output its associated sport label. We construct two types of demonstrations: *identifying*, where the sport is a distinctive national or traditional sport that strongly pins down a unique rule, and *ambiguous*, where the sport is related to the country but can be explained by multiple plausible latent rules, providing weaker evidence about which rule the prompt instantiates. **(Task 2. Person Identification)** Given a company, the task is to output a canonical person name associated with that company. Similarly, we construct *identifying* demonstrations, where the person is an unambiguous representative that uniquely identifies the company, and *ambiguous* demonstrations, where the person is associated with the company but does not exclusively identify it. For both tasks, we sample $k \in \{2, 4, 8\}$ demonstrations from the corresponding pool and evaluate on a fixed test set. **(Results)** As shown in Tables 2–3, the identifying pool consistently yields higher accuracy than the ambiguous pool across both tasks and models (Qwen-235B-A22B and Qwen-30B-A3B), and the performance gap generally widens as the number of demonstrations increases. This confirms that more informative demonstrations lead to stronger task identification and better in-context generalization, consistent with our theoretical predictions. Additional dataset details and full evaluation results are provided in Appendix H.2.

5.2 Effect of Task Decomposition Quality in CoT

In Theorem 3.1, we show that the CoT performance depends on the subtask selection, or task decomposition. If we decompose the task into easier subtasks, CoT improves ICL performance; otherwise, it could be worse. We design a synthetic experiment to validate the implication.

(Setup) We perform two-stage training for Llama3.2-3B using LoRA. We first train the model on 20K six-digit addition samples, while the pretrained model already performs one- to

Table 1: **Test accuracy (\uparrow) of ICL under ambiguous and identifying demonstrations ($k = 8$).** Identifying demonstrations consistently yield higher accuracy across both tasks and models, indicating more precise task identification and better in-context generalization.

Task	Demonstration	Qwen-30B-A3B	Qwen-235B-A22B
Sport	Ambiguous	0.164 ± 0.039	0.202 ± 0.037
	Identifying	0.559 ± 0.074	0.602 ± 0.043
People	Ambiguous	0.820 ± 0.027	0.648 ± 0.008
	Identifying	0.990 ± 0.001	0.845 ± 0.044

five-digit addition and simple multiplication reliably. Our goal is to enable seven-digit addition via CoT prompting. To this end, we consider two decomposition strategies: (i) *In-Distribution Decomposition*, which decomposes the task into sub-computations the model has already mastered, namely six-digit addition, a one-digit addition, and a simple multiplication by 10; (ii) *Out-of-Distribution Decomposition*, which decomposes the task into intermediate steps that still require seven-digit addition, effectively preserving the original difficulty and introducing sub-tasks the model cannot reliably solve in isolation. We construct a second training set of 500K samples using the in-distribution decomposition strategy, and evaluate the model under both decomposition strategies, with prompts containing zero to five demonstrations. **(Results)** Results are shown in Figure 1b. In-distribution decomposition substantially improves performance, whereas out-of-distribution decomposition performs worse than vanilla ICL without CoT and degrades further as the number of demonstrations increases. This behavior supports our result in Theorem 3.1. Prompt templates and additional experimental details are provided in Appendix H.4.

5.3 Prompt Sensitivity vs. Demonstration Count

In Section 4, Theorems 4.3 and 4.7 show that prompt templates exhibit different synergy with demonstration count in ICL. For prompt formats 1–5, as the number of demonstrations increases, ICL performance becomes less sensitive to the instruction. In contrast, for prompt 6, where all instructions are incorrect and different, prompt sensitivity persists even with many demonstrations. We design the following experiment to validate this insight.

(Setup) We use a pretrained Qwen3-235B-A22B model and consider three prompt formats: prompt 3 and prompt 5 from Theorem 4.3, and prompt 6 from Theorem 4.7. We focus on the three-digit addition task. For prompt 3, we use the correct operator $+$ in all demonstrations and test queries. For prompt 5, we replace all $+$ symbols with \times , while keeping the demonstration outputs as sums, requiring the model to infer the true task from examples. For prompt 6, we randomly replace $+$ with \times , $/$, or $-$ for all demonstrations, introducing fully incorrect and inconsistent instructions. **(Results)** We evaluate the model under the three prompt formats with 1 to 50 demonstrations. We visualize the gradient of the output logits with respect to the instruction tokens in Figure 1c. For prompt 3, the gradient remains near zero throughout, indicating low instruction sensitivity. For prompt 5, instruction sensitivity is initially high, reflecting a bias toward multiplication, and gradually decreases as the model infers the correct task from demonstrations. In contrast, for prompt 6, the gradient magnitude increases with more demonstrations, indicating persistent and even amplified instruction sensitivity. These observations are consistent with our theoretical analysis. Additional settings and results are provided in Appendix H.3.

6 Conclusion

In this work, we characterize in-context-learning (ICL) performance in terms of the intrinsic capability, the distance between test and pretraining prompts, and the task-identification power of demonstrations. Specifically, we show that effective demonstrations correspond to low-Lipschitz paths that reliably identify the underlying task, whereas poorly chosen demonstrations or format variations can destabilize ICL by inducing perturbations. We also establish bounds showing that, under task-consistent prompts, the influence of instructions vanishes as the number of demonstrations increases, whereas inconsistent demonstrations or format variations prevent task identification. We further extend the analysis to CoT by treating multi-step reasoning as a sequence of task-identification steps and deriving conditions under which this decomposition remains stable. Our paper develops a theoretical framework to analyze how the relationship between prompts and pre-training data affects the quality of in-context learning. This lays a theoretical foundation for further research on prompting, including topics such as hallucination and security.

References

- Rishabh Agarwal, Avi Singh, Lei Zhang, Bernd Bohnet, Luis Rosias, Stephanie Chan, Biao Zhang, Ankesh Anand, Zaheer Abbas, Azade Nova, John D. Co-Reyes, Eric Chu, Feryal Behbahani, Aleksandra Faust, and Hugo Larochelle. Many-shot in-context learning. *Advances in Neural Information Processing Systems*, 37:76930–76966, 2024.
- Kwangjun Ahn, Xiang Cheng, Hadi Daneshmand, and Suvrit Sra. Transformers learn to implement preconditioned gradient descent for in-context learning. *Advances in Neural Information Processing Systems*, 36, 2023.
- Ekin Akyürek, Dale Schuurmans, Jacob Andreas, Tengyu Ma, and Denny Zhou. What learning algorithm is in-context learning? investigations with linear models. *International Conference on Learning Representations*, 2023.
- Yu Bai, Fan Chen, Huan Wang, Caiming Xiong, and Song Mei. Transformers as statisticians: Provable in-context learning with in-context algorithm selection. In *Thirty-seventh Conference on Neural Information Processing Systems*, 2023.
- Tom Brown, Benjamin Mann, Nick Ryder, Melanie Subbiah, Jared D Kaplan, Prafulla Dhariwal, Arvind Neelakantan, Pranav Shyam, Girish Sastry, Amanda Askell, et al. Language models are few-shot learners. *Advances in neural information processing systems*, 33:1877–1901, 2020.
- Mark Chen. Evaluating large language models trained on code. *arXiv preprint arXiv:2107.03374*, 2021.
- Karl Cobbe, Vineet Kosaraju, Mohammad Bavarian, Mark Chen, Heewoo Jun, Lukasz Kaiser, Matthias Plappert, Jerry Tworek, Jacob Hilton, Reiichiro Nakano, et al. Training verifiers to solve math word problems. *arXiv preprint arXiv:2110.14168*, 2021.
- Yingqian Cui, Pengfei He, Xianfeng Tang, Qi He, Chen Luo, Jiliang Tang, and Yue Xing. A theoretical understanding of chain-of-thought: Coherent reasoning and error-aware demonstration. In *The 28th International Conference on Artificial Intelligence and Statistics*, 2025.

- Damai Dai, Yutao Sun, Li Dong, Yaru Hao, Shuming Ma, Zhifang Sui, and Furu Wei. Why can gpt learn in-context? language models implicitly perform gradient descent as meta-optimizers. *ICLR 2023 Workshop on Mathematical and Empirical Understanding of Foundation Models*, 2023.
- Nelson Elhage, Neel Nanda, Catherine Olsson, Tom Henighan, Nicholas Joseph, Ben Mann, Amanda Askell, Yuntao Bai, Anna Chen, Tom Conerly, Nova DasSarma, Dawn Drain, Deep Ganguli, Zac Hatfield-Dodds, Danny Hernandez, Andy Jones, Jackson Kernion, Liane Lovitt, Kamal Ndousse, Dario Amodei, Tom Brown, Jack Clark, Jared Kaplan, Sam McCandlish, and Chris Olah. A mathematical framework for transformer circuits. *Transformer Circuits Thread*, 2021.
- Guhao Feng, Bohang Zhang, Yuntian Gu, Haotian Ye, Di He, and Liwei Wang. Towards revealing the mystery behind chain of thought: A theoretical perspective. *Advances in Neural Information Processing Systems*, 2023.
- Deqing Fu, Tian-Qi Chen, Robin Jia, and Vatsal Sharan. Transformers learn to achieve second-order convergence rates for in-context linear regression. *Advances in Neural Information Processing Systems*, 37:98675–98716, 2024.
- Angeliki Giannou, Shashank Rajput, and Dimitris Papailiopoulos. The expressive power of tuning only the normalization layers. In *Proceedings of Thirty Sixth Conference on Learning Theory*, volume 195, pages 4130–4131, 2023.
- Zixuan Gong, Xiaolin Hu, Huayi Tang, and Yong Liu. Towards auto-regressive next-token prediction: In-context learning emerges from generalization. In *The Thirteenth International Conference on Learning Representations*, 2025. URL <https://openreview.net/forum?id=gK1rl98VRp>.
- Jianliang He, Xintian Pan, Siyu Chen, and Zhuoran Yang. In-context linear regression demystified: Training dynamics and mechanistic interpretability of multi-head softmax attention. In *Forty-second International Conference on Machine Learning*, 2025. URL <https://openreview.net/forum?id=3TM3fxwTps>.
- Dan Hendrycks, Collin Burns, Steven Basart, Andy Zou, Mantas Mazeika, Dawn Song, and Jacob Steinhardt. Measuring massive multitask language understanding. In *International Conference on Learning Representations*, 2021a.
- Dan Hendrycks, Collin Burns, Saurav Kadavath, Akul Arora, Steven Basart, Eric Tang, Dawn Song, and Jacob Steinhardt. Measuring mathematical problem solving with the MATH dataset. In *Thirty-fifth Conference on Neural Information Processing Systems Datasets and Benchmarks Track (Round 2)*, 2021b.
- Juno Kim and Taiji Suzuki. Transformers learn nonlinear features in context. In *ICLR 2024 Workshop on Mathematical and Empirical Understanding of Foundation Models*, 2024. URL <https://openreview.net/forum?id=WvvAu6XI1M>.
- Juno Kim, Tai Nakamaki, and Taiji Suzuki. Transformers are minimax optimal nonparametric in-context learners, 2024. URL <https://arxiv.org/abs/2408.12186>.
- Takeshi Kojima, Shixiang Shane Gu, Machel Reid, Yutaka Matsuo, and Yusuke Iwasawa. Large language models are zero-shot reasoners, 2023. URL <https://arxiv.org/abs/2205.11916>.
- Hongbo Li, Lingjie Duan, and Yingbin Liang. Provable in-context learning of nonlinear regression with transformers, 2025. URL <https://arxiv.org/abs/2507.20443>.

- Yingcong Li, Kartik Sreenivasan, Angeliki Giannou, Dimitris Papailiopoulos, and Samet Oymak. Dissecting chain-of-thought: Compositionality through in-context filtering and learning. In *Thirty-seventh Conference on Neural Information Processing Systems*, 2023. URL <https://openreview.net/forum?id=xEhKwsqxMa>.
- Zhiyuan Li, Hong Liu, Denny Zhou, and Tengyu Ma. Chain of thought empowers transformers to solve inherently serial problems. *International Conference on Learning Representations*, 2024.
- Jiachang Liu, Dinghan Shen, Yizhe Zhang, William B. Dolan, Lawrence Carin, and Weizhu Chen. What makes good in-context examples for gpt-3? *Proceedings of Deep Learning Inside Out (DeeLIO 2022): The 3rd Workshop on Knowledge Extraction and Integration for Deep Learning Architectures*, pages 100–114, 2022.
- G. G Lorentz. *Approximation of functions*. Chelsea Pub. Co., New York, N.Y., 1986.
- Fei Lu and Yue Yu. Transformer learns the cross-task prior and regularization for in-context learning, 2025. URL <https://arxiv.org/abs/2505.12138>.
- Arvind V. Mahankali, Tatsunori Hashimoto, and Tengyu Ma. One step of gradient descent is provably the optimal in-context learner with one layer of linear self-attention. In *The Twelfth International Conference on Learning Representations*, 2024.
- William Merrill and Ashish Sabharwal. The expressive power of transformers with chain of thought. *International Conference on Learning Representations*, 2024.
- Sewon Min, Xinxu Lyu, Ari Holtzman, Mikel Artetxe, Mike Lewis, Hannaneh Hajishirzi, and Luke Zettlemoyer. Rethinking the role of demonstrations: What makes in-context learning work? *Empirical Methods in Natural Language Processing*, 2022.
- Maxwell Nye, Anders Johan Andreassen, Guy Gur-Ari, Henryk Michalewski, Jacob Austin, David Bieber, David Dohan, Aitor Lewkowycz, Maarten Bosma, David Luan, Charles Sutton, and Augustus Odena. Show your work: Scratchpads for intermediate computation with language models, 2021. URL <https://arxiv.org/abs/2112.00114>.
- Kazusato Oko, Yujin Song, Taiji Suzuki, and Denny Wu. Pretrained transformer efficiently learns low-dimensional target functions in-context. *Advances in Neural Information Processing Systems*, 37:77316–77365, 2024.
- Catherine Olsson, Nelson Elhage, Neel Nanda, Nicholas Joseph, Nova DasSarma, Tom Henighan, Ben Mann, Amanda Askell, Yuntao Bai, Anna Chen, Tom Conerly, Dawn Drain, Deep Ganguli, Zac Hatfield-Dodds, Danny Hernandez, Scott Johnston, Andy Jones, Jackson Kernion, Liane Lovitt, Kamal Ndousse, Dario Amodei, Tom Brown, Jack Clark, Jared Kaplan, Sam McCandlish, and Chris Olah. In-context learning and induction heads, 2022. URL <https://arxiv.org/abs/2209.11895>.
- OpenAI. Gpt-4 technical report. *arXiv preprint arXiv:2303.08774*, 2023.
- Madhur Panwar, Kabir Ahuja, and Navin Goyal. In-context learning through the bayesian prism. In *The Twelfth International Conference on Learning Representations*, 2024. URL <https://openreview.net/forum?id=HX5ujdsSon>.

- David Rein, Betty Li Hou, Asa Cooper Stickland, Jackson Petty, Richard Yuanzhe Pang, Julien Dirani, Julian Michael, and Samuel R. Bowman. GPQA: A graduate-level google-proof q&a benchmark. In *First Conference on Language Modeling*, 2024. URL <https://openreview.net/forum?id=Ti67584b98>.
- Evgeny J. Remez. Sur une propriété extrême des polynômes de tchebychef. *Communications de l'Institut des Sciences Mathématiques et Mécaniques de l'Université de Kharkoff*, 13:93–95, 1936.
- Hongjin Su, Jungo Kasai, Chen Henry Wu, Weijia Shi, Tianlu Wang, Jiayi Xin, Rui Zhang, Mari Ostendorf, Luke Zettlemoyer, Noah A. Smith, and Tao Yu. Selective annotation makes language models better few-shot learners. In *The Eleventh International Conference on Learning Representations*, 2023.
- Eric Todd, Millicent L. Li, Arnab Sen Sharma, Aaron Mueller, Byron C. Wallace, and David Bau. Function vectors in large language models, 2024. URL <https://arxiv.org/abs/2310.15213>.
- Rasul Tutunov, Antoine Grosnit, Juliusz Ziomek, Jun Wang, and Haitham Bou-Ammar. Why can large language models generate correct chain-of-thoughts?, 2024. URL <https://arxiv.org/abs/2310.13571>.
- Johannes von Oswald, Eyvind Niklasson, Ettore Randazzo, João Sacramento, Alexander Mordvintsev, Andrey Zhmoginov, and Max Vladymyrov. Transformers learn in-context by gradient descent. *International Conference on Machine Learning*, 2023.
- Xinyi Wang, Wanrong Zhu, and William Yang Wang. Large language models are implicitly topic models: Explaining and finding good demonstrations for in-context learning. *arXiv preprint arXiv:2301.11916*, 2023.
- Albert Webson and Ellie Pavlick. Do prompt-based models really understand the meaning of their prompts? In Marine Carpuat, Marie-Catherine de Marneffe, and Ivan Vladimir Meza Ruiz, editors, *Proceedings of the 2022 Conference of the North American Chapter of the Association for Computational Linguistics: Human Language Technologies*, pages 2300–2344, Seattle, United States, July 2022. Association for Computational Linguistics. doi: 10.18653/v1/2022.naacl-main.167. URL <https://aclanthology.org/2022.naacl-main.167/>.
- Jason Wei, Xuezhi Wang, Dale Schuurmans, Maarten Bosma, Brian Ichter, Fei Xia, Ed H. Chi, Quoc V. Le, and Denny Zhou. Chain-of-thought prompting elicits reasoning in large language models. *Advances in neural information processing systems*, 35:24824–24837, 2022.
- Don R. Wilhelmsen. A markov inequality in several dimensions. *Journal of Approximation Theory*, 11(3):216–220, 1974. ISSN 0021-9045. doi: [https://doi.org/10.1016/0021-9045\(74\)90012-4](https://doi.org/10.1016/0021-9045(74)90012-4). URL <https://www.sciencedirect.com/science/article/pii/0021904574900124>.
- Sang Michael Xie, Aditi Raghunathan, Percy Liang, and Tengyu Ma. An explanation of in-context learning as implicit bayesian inference. *International Conference on Learning Representations*, 2022.
- Chenxiao Yang, Zhiyuan Li, and David Wipf. An in-context learning theoretic analysis of chain-of-thought. In *ICML 2024 Workshop on In-Context Learning*, 2024a.
- Tong Yang, Yu Huang, Yingbin Liang, and Yuejie Chi. In-context learning with representations: Contextual generalization of trained transformers. In *The Thirty-eighth Annual Conference on Neural Information Processing Systems*, 2024b.

- Seonghyeon Ye, Hyeonbin Hwang, Sohee Yang, Hyeongu Yun, Yireun Kim, and Minjoon Seo. Investigating the effectiveness of task-agnostic prefix prompt for instruction following. In *Proceedings of the AAAI Conference on Artificial Intelligence*, volume 38, pages 19386–19394, 2024.
- Chulhee Yun, Srinadh Bhojanapalli, Ankit Singh Rawat, Sashank J. Reddi, and Sanjiv Kumar. Are transformers universal approximators of sequence-to-sequence functions? *International Conference on Learning Representations*, 2020.
- Yuchen Zeng and Kangwook Lee. The expressive power of low-rank adaptation. In *The Twelfth International Conference on Learning Representations*, 2024.
- Ruiqi Zhang, Spencer Frei, and Peter L. Bartlett. Trained transformers learn linear models in-context, 2023. URL <https://arxiv.org/abs/2306.09927>.
- Ruiqi Zhang, Spencer Frei, and Peter L. Bartlett. Trained transformers learn linear models in-context. *Journal of Machine Learning Research*, 25(49):1–55, 2024.
- Zihao Zhao, Eric Wallace, Shi Feng, Dan Klein, and Sameer Singh. Calibrate before use: Improving few-shot performance of language models. *International Conference on Machine Learning*, 139: 12697–12706, 2021.

Contents

1	Introduction	1
2	Lipschitz Characterization of Demonstration Effectiveness in ICL	3
2.1	Background	3
2.2	Lipschitz Generalization Bound	4
3	CoT in ICL: A Lipschitz-Based Perspective	6
3.1	Problem Setup	6
3.2	ICL Generalization Bound in the Presence of CoT	6
4	Synergistic Effects of Demonstration Count and Prompt Templates in ICL	7
4.1	Problem Setup	7
4.2	When Sensitivity to Prompt Templates Vanishes with Demonstrations	9
4.3	When Sensitivity to Prompt Templates Does not Vanishes with Demonstrations	10
5	Experiments	12
5.1	Quantifying Demonstration Effectiveness under Prompt Shift	12
5.2	Effect of Task Decomposition Quality in CoT	12
5.3	Prompt Sensitivity vs. Demonstration Count	13
6	Conclusion	14
A	List of Common Notations	21
B	Related Work	22
C	Proof of Theorem 2.3	24
C.1	Preliminaries	24
C.2	Proof of Theorem 2.3	25
D	Formal Justification of the Padding Reduction	26
D.1	Preliminaries	26
D.2	Stability of the Transformer Under Padding	27
E	Proof of Theorem 3.1	28
E.1	Preliminaries	28
E.2	Proof of Theorem E.5	30
E.3	Models can ignore irrelevant steps in CoT	31
F	Proof of Theorem 4.3, Corollary 4.4 and 4.5	31
F.1	Preliminaries	31
F.2	Proof of Theorem 4.3	34
F.3	Proof of Corollary 4.4	35
F.4	Proof of Corollary 4.5	36

G	Proof of Theorem 4.7 and Corollary 4.8	37
G.1	Preliminaries	38
G.2	Proof of Theorem 4.7	40
G.3	Proof of Corollary 4.8	41
H	Experiments	42
H.1	Pretraining Dependence	42
H.2	Demonstration Choice	43
H.3	Prompt Sensitivity vs. Demonstration Count	44
H.4	CoT Effect	44

A List of Common Notations

We summarize the main notations used throughout the paper and appendix for reference.

- \mathcal{V} : finite vocabulary.
- \mathcal{V}^* : set of all sequences of bounded length over \mathcal{V} .
- \mathcal{M} : class of Transformer models.
- $M \in \mathcal{M}$: pretrained Transformer model.
- M^* : target (oracle) model.
- z : a test prompt.
- $z^{(k)}$: prompt at CoT step k .
- $z^{*(k)}$: oracle rollout prompt at step k .
- D : ICL prompt domain. Throughout the paper, we assume that D is compact.
- D_0 : pretraining prompt domain.
- $D_0^{(k)}$: pretraining prompt domain for step- k CoT subtask.
- (x, y) : input-output pair.
- x_{query} : query input in the prompt.
- y_{query} : model output for the query.
- $\ell_{\text{ICL}}(z)$: ICL loss, defined as

$$\ell_{\text{ICL}}(z) := |M(z) - M^*(z)|.$$
- $\gamma(t)$: straight-line path between prompts, $t \in [0, 1]$.
- $\ell_{\text{ICL}}^\gamma(t)$: loss restricted to path γ .
- $L_{z, z'}$: Lipschitz constant of ℓ_{ICL} on a compact set containing the path between z and z' .
- L_γ : pathwise Lipschitz constant of path γ .
- J_γ : interval induced by D along path γ .
- E_γ : interval induced by D_0 along path γ .
- $\text{mes}(\cdot)$: Lebesgue measure.
- \mathcal{T} : finite latent task set.
- t^* : true latent task.
- $\pi(t)$: prior over tasks.
- $p(t | z)$: posterior distribution over tasks.

- $p(y_{\text{query}} | z)$: posterior predictive distribution.
- f_t : task-specific input-output mapping.
- i : instruction (or instruction sequence).
- D_i : extended instruction domain.
- D_{i0} : inner instruction domain (formats 1–5).
- B_r, B_R : Euclidean balls with radius r and R .
- L_i : instruction-Lipschitz constant.
- ∇_i : gradient with respect to instruction variables.
- K : number of CoT steps.
- L_k^* : Lipschitz constant of the oracle model at step k .
- $B_n f$: degree- n Bernstein polynomial approximation of f .
- C_γ : Remez amplification constant along path γ .
- C_V : Uniform constant only depending on the model structure.
- z_{pad} : padded prompt with special tokens.
- z_{orig} : original prompt without padding.

B Related Work

Existing theories rely on strong assumptions. A substantial body of theoretical work seeks to understand the mechanisms underlying ICL by analyzing how transformers implement learning procedures over context. At the mechanistic level, studies identify specific architectural patterns such as induction heads and function vectors—that enable example reuse and pattern matching across the context (Olsson et al., 2022; Elhage et al., 2021; Todd et al., 2024). Complementary algorithmic analyses show that, under linear or kernelized assumptions, ICL can be interpreted as implicitly gradient descent or kernel regression in activation space (Akyürek et al., 2023; von Oswald et al., 2023; Ahn et al., 2023; Mahankali et al., 2024), or as a form of task selection induced by the prior over pretraining tasks (Bai et al., 2023). While these mechanistic and algorithmic perspectives have significantly advanced our understanding of how ICL is computed, they typically rely on restrictive architectural assumptions, such as linear attention, single-layer or attention-only transformers, or single-head attention—and on idealized data distributions such as random generalized linear regression, which abstract away properties that are critical in practice (von Oswald et al., 2023; Mahankali et al., 2024; Zhang et al., 2024). A complementary line of work adopts a Bayesian or statistical inference perspective, interpreting ICL as approximate posterior inference over latent tasks conditioned on in-context demonstrations (Xie et al., 2022; Wang et al., 2023; Panwar et al., 2024). This framing provides a principled account of how generalization improves with more demonstrations, and has been extended to study the effects of noise, misspecification, and pretraining bias on ICL behavior (Gong et al., 2025). However, existing analyses within this framework uniformly assume a fixed and canonical context format, treating demonstrations as drawn from a coherent, well-specified data-generating process. As a result, they do not characterize how ICL behaves when the format of the context itself varies—a limitation that our work directly addresses.

Practical factors affect ICL generalization. Beyond mechanistic and statistical accounts, a large body of empirical work investigates how practical design choices in prompt construction affect ICL performance. A first line of work focuses on the role of demonstrations themselves: studies show that the number of demonstrations, their selection strategy, and the correctness of their labels each substantially influence downstream performance (Agarwal et al., 2024; Liu et al., 2022; Su et al., 2023). Notably, Min et al. (2022) find that label correctness in demonstrations matters less than expected, suggesting that ICL generalizes by retrieving a latent task structure rather than learning directly from individual examples. A second line of work examines chain-of-thought prompting, showing that including intermediate reasoning steps in demonstrations can dramatically improve performance on complex tasks (Wei et al., 2022; Kojima et al., 2023; Nye et al., 2021). Subsequent theoretical work explains CoT’s benefit in terms of expressivity: CoT enables deeper computation without additional layers (Feng et al., 2023), expands the model’s recognition capacity for complex problem classes (Merrill and Sabharwal, 2024), or supports more serial computation than standard forward passes allow (Li et al., 2024). However, these expressivity-based accounts do not characterize how CoT-structured demonstrations affect ICL generalization as the number of reasoning steps grows, which is a gap our work addresses through a multi-step error propagation analysis. A third line of work studies sensitivity to prompt format and template design, finding that surface-level variations in instruction wording, demonstration ordering, and label presentation can lead to large performance swings (Ye et al., 2024; Zhao et al., 2021; Webson and Pavlick, 2022). Despite the breadth of these empirical findings, they remain largely descriptive: existing work does not provide a theoretical criterion for when format variation preserves successful generalization and when it fundamentally disrupts consistent task inference. Our work provides such a criterion by formally distinguishing prompt formats under which the posterior predictive converges exponentially with more demonstrations from those under which convergence necessarily fails.

Mechanistic explanations of ICL. A complementary line of work try to explain ICL at the level of internal representations and computational mechanisms, examining how specific architectural components give rise to in-context behavior. At the representational level, studies identify induction heads and function vectors as key circuits that enable pattern matching and example reuse across the context window (Olsson et al., 2022; Elhage et al., 2021; Todd et al., 2024), and related work shows that multi-head softmax attention can implement regression behaviors in simplified settings (He et al., 2025; Li et al., 2025). At the algorithmic level, several studies argue that transformers implicitly perform gradient descent or kernel regression over in-context examples (Akyürek et al., 2023; von Oswald et al., 2023; Ahn et al., 2023), and related perspectives characterize ICL as algorithm selection or prior-induced regularization across tasks (Bai et al., 2023; Lu and Yu, 2025). A separate line of work examines whether standard pretraining objectives can produce the representational capacity assumed by these accounts, establishing conditions under which pretrained transformers exhibit ICL-like behavior (Kim and Suzuki, 2024; Kim et al., 2024). While these mechanistic and algorithmic explanations have significantly advanced our understanding of the computational substrate of ICL, they characterize how ICL is implemented within a fixed architecture and format, but do not address when and why ICL generalizes across varying prompt formats, nor how practical design choices such as demonstration count, CoT structure, or instruction variation affect the quality of task inference. Our work is therefore complementary to this line, operating at the level of generalization theory rather than mechanistic realization.

C Proof of Theorem 2.3

In this appendix, we provide a complete proof of the formal Lipschitz generalization bound stated in Section 2.

C.1 Preliminaries

We first introduce Bernstein polynomials here, which we will use to construct polynomial surrogates for the path-restricted loss. Detailed properties of Bernstein polynomials can be found in [Lorentz \(1986\)](#).

For a function $f : [0, 1] \rightarrow \mathbb{R}$ and an integer $n \geq 1$, its degree- n Bernstein polynomial is defined by

$$B_n f(t) = \sum_{k=0}^n f\left(\frac{k}{n}\right) \binom{n}{k} t^k (1-t)^{n-k}, \quad t \in [0, 1].$$

The function $B_n f$ is a polynomial of degree at most n . Moreover, if f is Lipschitz continuous with constant l on $[0, 1]$, then (see [Lemma 2.2](#))

$$\sup_{t \in [0, 1]} |B_n f(t) - f(t)| \leq \frac{l}{2\sqrt{n}}.$$

The proof relies on two standard tools from approximation theory: the Bernstein polynomial approximation theorem and the Remez inequality. For completeness, we briefly recall their statements in the form needed here.

Lemma C.1 (Remez Inequality for Polynomials ([Remez, 1936](#))). *If $J \in \mathbb{R}$ is a finite interval, and $E \subset J$ is an arbitrary measurable set, then for any polynomial p of degree n ,*

$$\max_{x \in J} |p(x)| \leq \left(\frac{4 \operatorname{mes}(J)}{\operatorname{mes}(E)} \right)^n \sup_{x \in E} |p(x)|.$$

Lemma C.2 (Bernstein Approximation Theorem, Lipschitz Case ([Lorentz, 1986](#))). *Let $f : [0, 1] \rightarrow \mathbb{R}$ be a Lipschitz continuous function with Lipschitz constant L . Let $B_n f$ denote the degree- n Bernstein polynomial (see [Appendix C](#) for definition) approximation of f . Then, for all $n \geq 1$,*

$$\sup_{x \in [0, 1]} |B_n f(x) - f(x)| \leq \frac{L}{2\sqrt{n}}.$$

We then introduce the assumptions required for the proof.

Assumption C.3 (Local Lipschitzness along paths). For every pair (z, z') considered, there exists a compact set $\mathcal{K}_{z, z'} \subset \mathcal{V}^*$ such that $\gamma([0, 1]) \subset \mathcal{K}_{z, z'}$ and the loss ℓ_{ICL} is Lipschitz on $\mathcal{K}_{z, z'}$ with constant $L_{z, z'} < \infty$:

$$|\ell_{\text{ICL}}(\mathbf{a}) - \ell_{\text{ICL}}(\mathbf{b})| \leq L_{z, z'} \|\mathbf{a} - \mathbf{b}\|, \quad \forall \mathbf{a}, \mathbf{b} \in \mathcal{K}_{z, z'}.$$

This assumption states that the loss varies in a controlled manner along any straight-line interpolation between a test prompt and a reference pretraining prompt. We only require Lipschitz continuity on a compact neighborhood of the path, rather than globally over \mathcal{V}^* . We perform the analysis in the continuous embedding representation space induced by the tokenizer and embedding layer. Although the token domain \mathcal{V}^* is discrete, its embedding representation lies in a continuous vector space, where the interpolation paths used in our proof are defined.

Recall that γ refers to the path between test prompt z and pretraining prompt z' , \mathbb{E}_γ refers to interval induced by D_0 along path γ .

Assumption C.4 (Positive pretraining coverage along a connecting path). There exist a point $\mathbf{z}' \in D_0$ and a continuous path $\gamma : [0, 1] \rightarrow D$ connecting \mathbf{z} and \mathbf{z}' (i.e., $\gamma(0) = \mathbf{z}$ and $\gamma(1) = \mathbf{z}'$) such that $\text{mes}(E_\gamma) > 0$.

This assumption ensures that the pretraining domain occupies a non-negligible portion of the interpolation path between \mathbf{z}' and \mathbf{z} . Equivalently, the model must have seen a positive-measure subset of prompts along the direction connecting the test prompt to the pretraining domain.

C.2 Proof of Theorem 2.3

We first present the formal statement of the Lipschitz generalization bound, which is a more detailed version of Theorem 2.3 in the main text.

Theorem C.5 (ICL Generalization Bound, formal version of Theorem 2.3). *Let $\mathbf{z} \notin D_0$ and suppose Assumptions C.3 and C.4 hold. Fix any $\mathbf{z}' \in D_0$ such that $\text{mes}(E_\gamma) > 0$ for the straight-line path $\gamma(t) = \mathbf{z}' + t(\mathbf{z} - \mathbf{z}')$. Let $l_\gamma := L_{\mathbf{z}, \mathbf{z}'} \|\mathbf{z} - \mathbf{z}'\|$ and*

$$A_\gamma := \frac{4 \text{mes}(J_\gamma)}{\text{mes}(E_\gamma)} > 1,$$

where $\text{mes}(J_\gamma)$ is a constant.

Then for any integer $n \geq 1$,

$$\ell_{ICL}(\mathbf{z}) \leq A_\gamma^n \sup_{\tilde{\mathbf{z}} \in D_0} \ell_{ICL}(\tilde{\mathbf{z}}) + \left(1 + A_\gamma^n\right) \frac{l_\gamma}{2\sqrt{n}}. \quad (4)$$

In particular, choosing $n = \lceil l_\gamma^2 \rceil$ yields

$$\ell_{ICL}(\mathbf{z}) \leq A_\gamma^{\lceil l_\gamma^2 \rceil} \sup_{\tilde{\mathbf{z}} \in D_0} \ell_{ICL}(\tilde{\mathbf{z}}) + \frac{1 + A_\gamma^{\lceil l_\gamma^2 \rceil}}{2}. \quad (5)$$

We now proceed with the proof, following the same four conceptual steps as outlined in the proof sketch.

Proof. Step 1: Reduce the prompt space to a finite interval via a path. Fix $\mathbf{z} \notin D_0$ and choose $\mathbf{z}' \in D_0$ such that $\text{mes}(E_\gamma) > 0$ for the path $\gamma(t) = \mathbf{z}' + t(\mathbf{z} - \mathbf{z}')$, $t \in [0, 1]$. Define the path-restricted loss

$$\ell_{ICL}^\gamma(t) := \ell_{ICL}(\gamma(t)), \quad t \in [0, 1].$$

By Assumption C.3, ℓ_{ICL} is Lipschitz on a compact set containing $\gamma([0, 1])$, hence for all $t_1, t_2 \in [0, 1]$,

$$|\ell_{ICL}^\gamma(t_1) - \ell_{ICL}^\gamma(t_2)| \leq L_{\mathbf{z}, \mathbf{z}'} \|\gamma(t_1) - \gamma(t_2)\| = L_{\mathbf{z}, \mathbf{z}'} \|\mathbf{z} - \mathbf{z}'\| |t_1 - t_2|.$$

Denote $l_\gamma := L_{\mathbf{z}, \mathbf{z}'} \|\mathbf{z} - \mathbf{z}'\|$.

We further denote the intervals induced along the path by

$$J_\gamma := [0, 1], \quad E_\gamma := \{t \in J_\gamma : \gamma(t) \in D_0\}.$$

By construction and Assumption C.4, $\text{mes}(E_\gamma) > 0$.

Step 2: Convert a Lipschitz function into a polynomial via Bernstein approximation.

Applying Lemma C.2 to the Lipschitz function ℓ_{ICL}^γ gives

$$\sup_{t \in [0, 1]} |B_n \ell_{ICL}^\gamma(t) - \ell_{ICL}^\gamma(t)| \leq \frac{l_\gamma}{2\sqrt{n}}.$$

Note that $B_n \ell_{\text{ICL}}^\gamma$ is a polynomial of degree at most n .

Step 3: Apply Remez–Chebyshev to the polynomial surrogate. Applying Lemma C.1 to $p = B_n \ell_{\text{ICL}}^\gamma$ on the interval J_γ with subset E_γ yields

$$\max_{t \in J_\gamma} |B_n \ell_{\text{ICL}}^\gamma(t)| \leq \left(\frac{4 \operatorname{mes}(J_\gamma)}{\operatorname{mes}(E_\gamma)} \right)^n \sup_{t \in E_\gamma} |B_n \ell_{\text{ICL}}^\gamma(t)|.$$

Denote $A_\gamma := \frac{4 \operatorname{mes}(J_\gamma)}{\operatorname{mes}(E_\gamma)}$.

Step 4: Transfer the bound back to ℓ_{ICL} and choose n . For any $t \in J_\gamma$,

$$\ell_{\text{ICL}}^\gamma(t) \leq B_n \ell_{\text{ICL}}^\gamma(t) + |B_n \ell_{\text{ICL}}^\gamma(t) - \ell_{\text{ICL}}^\gamma(t)| \leq B_n \ell_{\text{ICL}}^\gamma(t) + \frac{l_\gamma}{2\sqrt{n}}.$$

Taking maxima over $t \in J_\gamma$ and using the Remez bound,

$$\max_{t \in J_\gamma} \ell_{\text{ICL}}^\gamma(t) \leq A_\gamma^n \sup_{t \in E_\gamma} B_n \ell_{\text{ICL}}^\gamma(t) + \frac{l_\gamma}{2\sqrt{n}}.$$

Moreover, for $t \in E_\gamma$,

$$B_n \ell_{\text{ICL}}^\gamma(t) \leq \ell_{\text{ICL}}^\gamma(t) + \frac{l_\gamma}{2\sqrt{n}}.$$

Combining the last two displays yields

$$\max_{t \in J_\gamma} \ell_{\text{ICL}}^\gamma(t) \leq A_\gamma^n \sup_{t \in E_\gamma} \ell_{\text{ICL}}^\gamma(t) + \left(1 + A_\gamma^n\right) \frac{l_\gamma}{2\sqrt{n}}.$$

Since $\gamma(t) \in D_0$ for $t \in E_\gamma$,

$$\sup_{t \in E_\gamma} \ell_{\text{ICL}}^\gamma(t) \leq \sup_{\tilde{z} \in D_0} \ell_{\text{ICL}}(\tilde{z}).$$

Finally, $\ell_{\text{ICL}}(\mathbf{z}) = \ell_{\text{ICL}}^\gamma(1) \leq \max_{t \in J_\gamma} \ell_{\text{ICL}}^\gamma(t)$, which proves (4). The specialization (5) follows by choosing $n = \lceil l_\gamma^2 \rceil$ and noting $l_\gamma/\sqrt{n} \leq 1$. \square

D Formal Justification of the Padding Reduction

D.1 Preliminaries

In this appendix, we justify the general padding assumption mentioned in Section 2.2, which is used throughout the analysis in Theorem 2.3 and Theorem 3.1. The purpose of padding is to align the effective input domain at inference with that of pretraining, without altering the underlying function class implemented by the model.

Definition of Padding In practice, prompts may have different lengths. To enable a unified functional analysis, we embed all prompts into a fixed-length space via padding. For any prompt \mathbf{z} , we define a padded version \mathbf{z}_{pad} obtained by inserting a special token $\langle \text{pad} \rangle$ at arbitrary positions, subject to the following constraints: the original non-padding tokens remain unchanged; their relative order is preserved; and only additional $\langle \text{pad} \rangle$ tokens are inserted. Without padding, prompts of varying lengths cannot be treated as elements of a common ambient space, precluding a unified functional analysis.

D.2 Stability of the Transformer Under Padding

Let y and y' denote the attention outputs at a fixed query position before and after adding padding tokens, respectively. Let z be the original prompt and z_{pad} be the padded prompt obtained by inserting m padding tokens without modifying any non-padding token. We assume that the embedding of $\langle \text{pad} \rangle$ is the zero vector, so that the input representations satisfy $z_{\text{pad}}^{(0)} = z^{(0)}$ at positions corresponding to original tokens. We show that, under mild conditions, the attention output is stable under padding: $\|y' - y\|_2$ can be made arbitrarily small by controlling (i) the number m of padding tokens and (ii) their relative attention logits.

Lemma D.1 (Attention Stability Under Padding). *Let y and y' denote the attention outputs before and after adding m padding tokens. Let x_i denote the attention score assigned to token i , x_p denote the attention score assigned to pad token p , respectively. Let z be the original prompt and z_{pad} be the padded prompt obtained by inserting m padding tokens. Then there exists a uniform constant C_V such that*

$$\|y' - y\|_2 \leq 2C_V \cdot \frac{z_{\text{pad}}}{z_{\text{orig}} + z_{\text{pad}}} \leq 2C_V \cdot \frac{m e^{x_{\text{pad}, \max}}}{z_{\text{orig}}}.$$

In particular, for any tolerance $\varepsilon \in (0, 2C_V)$, the condition

$$m \leq \frac{\varepsilon}{2C_V - \varepsilon} e^{\Delta}$$

is sufficient to ensure $\|y' - y\|_2 \leq \varepsilon$, where $j \in \mathcal{I}$ indexes a dominant informative token, and $\Delta := x_j - x_{\text{pad}, \max}$ denotes the softmax gap between informative and padding tokens.

Proof. We use the standard attention form at a fixed query position:

$$y = \frac{1}{z_{\text{orig}}} \sum_{i \in \mathcal{I}} e^{x_i} v_i, \quad y' = \frac{1}{z_{\text{orig}} + z_{\text{pad}}} \left(\sum_{i \in \mathcal{I}} e^{x_i} v_i + \sum_{p \in \mathcal{P}} e^{x_p} v_p \right),$$

where

$$z_{\text{orig}} := \sum_{i \in \mathcal{I}} e^{x_i}, \quad z_{\text{pad}} := \sum_{p \in \mathcal{P}} e^{x_p}.$$

Subtracting y from y' gives

$$y' - y = \frac{\sum_{p \in \mathcal{P}} e^{x_p} v_p}{z_{\text{orig}} + z_{\text{pad}}} - \frac{z_{\text{pad}}}{z_{\text{orig}}(z_{\text{orig}} + z_{\text{pad}})} \sum_{i \in \mathcal{I}} e^{x_i} v_i.$$

Taking ℓ_2 norms and using the triangle inequality,

$$\|y' - y\|_2 \leq \frac{\left\| \sum_{p \in \mathcal{P}} e^{x_p} v_p \right\|_2}{z_{\text{orig}} + z_{\text{pad}}} + \frac{z_{\text{pad}} \left\| \sum_{i \in \mathcal{I}} e^{x_i} v_i \right\|_2}{z_{\text{orig}}(z_{\text{orig}} + z_{\text{pad}})}.$$

Let C_V be a uniform upper bound on $\|v_i\|_2$. Then

$$\left\| \sum_{p \in \mathcal{P}} e^{x_p} v_p \right\|_2 \leq C_V z_{\text{pad}}, \quad \left\| \sum_{i \in \mathcal{I}} e^{x_i} v_i \right\|_2 \leq C_V z_{\text{orig}}.$$

Substituting yields

$$\|y' - y\|_2 \leq 2C_V \frac{z_{\text{pad}}}{z_{\text{orig}} + z_{\text{pad}}}.$$

Let

$$x_{\text{pad,max}} := \max_{p \in \mathcal{P}} x_p$$

denote the maximum attention logit assigned to any padding token, we further obtain

$$\|y' - y\|_2 \leq 2C_V \frac{me^{x_{\text{pad,max}}}}{z_{\text{orig}}},$$

which establishes the first two inequalities in the lemma statement.

For the sufficient condition, solving

$$2C_V \frac{z_{\text{pad}}}{z_{\text{orig}} + z_{\text{pad}}} \leq \varepsilon$$

gives

$$z_{\text{pad}} \leq \frac{\varepsilon}{2C_V - \varepsilon} z_{\text{orig}}.$$

If there exists $j \in \mathcal{I}$ such that $\Delta = x_j - x_{\text{pad,max}} > 0$, then

$$z_{\text{pad}} \leq me^{x_{\text{pad,max}}} = me^{x_j - \Delta}, \quad z_{\text{orig}} \geq e^{x_j}.$$

Hence

$$\frac{z_{\text{pad}}}{z_{\text{orig}}} \leq me^{-\Delta}.$$

Imposing

$$m \leq e^{\Delta} \frac{\varepsilon}{2C_V - \varepsilon}$$

yields the stated sufficient condition. \square

Lemma D.1 shows that padding tokens act as structured distractors whose only influence on the attention output is through their contribution to the softmax normalization mass. The perturbation does not depend on the semantic content of the padding tokens themselves, but is governed entirely by two quantitative factors: (i) the number m of padding tokens and (ii) their relative attention logits compared to informative tokens. More precisely, the stability bound depends on the quantity $me^{-\Delta}$, where Δ denotes the softmax gap between a dominant informative token and the most competitive padding token. Thus, stability is ensured either when the padding length m is controlled, or when padding tokens receive sufficiently small attention scores (i.e., when Δ is large).

E Proof of Theorem 3.1

In this appendix we provide a complete proof of the multi-step error propagation bound underlying Section 3.

E.1 Preliminaries

We briefly recall the main objects appearing in the multi-step CoT analysis and define new notations essential for the proof.

- Let $(\mathcal{Z}, \|\cdot\|)$ be the prompt space. For a fixed initial prompt $\mathbf{z}^{(0)}$, define the model and oracle rollouts by

$$\mathbf{z}^{(k+1)} = f(\mathbf{z}^{(k)}, M(\mathbf{z}^{(k)})), \quad \mathbf{z}^{*(k+1)} = f(\mathbf{z}^{*(k)}, M_{\star}(\mathbf{z}^{*(k)})),$$

with $\mathbf{z}^{*(0)} = \mathbf{z}^{(0)}$, where $f(\mathbf{z}, a)$ denotes the operation of appending answer a to prompt \mathbf{z} .

- The learned model is denoted by $M : \mathcal{Z} \rightarrow \mathbb{R}$, and the reference (oracle) predictor is denoted by $M_\star : \mathcal{Z} \rightarrow \mathbb{R}$. We define the single-step prediction error as

$$\ell_{\text{ICL}}(\mathbf{z}) := |M(\mathbf{z}) - M_\star(\mathbf{z})|.$$

- We measure the discrepancy between the model and oracle rollouts by

$$\Delta_k := \|\mathbf{z}^{(k)} - \mathbf{z}^{\star(k)}\|, \quad \Delta_0 = 0.$$

We then introduce the assumptions and lemmas required for the proof.

Assumption E.1. Both sequences are well-defined for $k = 0, \dots, K - 2$ and remain in \mathcal{Z} .

Assumption E.2 (Per-step error propagation). For each step $k \in \{0, \dots, K - 2\}$, there exist constants $\alpha_k, \beta_k \geq 0$ such that

$$\Delta_{k+1} \leq \beta_k \ell_{\text{ICL}}(\mathbf{z}^{(k)}) + \alpha_k \Delta_k.$$

This assumption captures how errors propagate through a single CoT step. The term $\beta_k \varepsilon(\mathbf{z}^{(k)})$ reflects direct error injection: even if the model and oracle rollouts are currently at the same state ($\Delta_k = 0$), a prediction error $\varepsilon(\mathbf{z}^{(k)})$ at step k will cause the two rollouts to diverge at step $k + 1$, with β_k measuring how sensitive the update f is to the predicted answer. The term $\alpha_k \Delta_k$ reflects error accumulation: any existing divergence Δ_k between the two rollouts is carried forward and potentially amplified by α_k , which captures the sensitivity of f to the current prompt state as well as how the oracle predictor’s smoothness interacts with the update.

Assumption E.3. For each step k , there exists a set \mathcal{R}_k containing all rollout states at step k such that M_\star is L_k^\star -Lipschitz on \mathcal{R}_k :

$$|M_\star(\mathbf{z}) - M_\star(\mathbf{z}')| \leq L_k^\star \|\mathbf{z} - \mathbf{z}'\|.$$

Lemma E.4. Fix a CoT step $k \in \{0, \dots, K - 1\}$. Let $\ell_{\text{ICL}}^k : \mathcal{Z} \rightarrow \mathbb{R}_+$ denote the step- k prediction error

$$\ell_{\text{ICL}}^k(\mathbf{z}) := |M(\mathbf{z}^{(k)}) - M_\star(\mathbf{z}^{(k)})|,$$

Assume the single-step Lipschitz generalization theorem (Theorem 2.3) holds when instantiated to this step- k subtask, with pretraining prompt set $D_0^{(k)} \subset \mathcal{Z}$. Then there exist constants $C_k \geq 1$ and an effective Lipschitz parameter $L_{(k)} \geq 0$ such that for any step- k rollout prompt $\mathbf{z}^{(k)} \notin D_0^{(k)}$,

$$\ell_{\text{ICL}}^k(\mathbf{z}^{(k)}) \leq C_k \exp(L_{(k)}^2) \cdot \sup_{\mathbf{z}' \in D_0^{(k)}} \ell_{\text{ICL}}^k(\mathbf{z}').$$

Proof. We apply Theorem 2.3 to the step- k subtask. Concretely, we view $\ell_{\text{ICL}}^k(\cdot)$ as the single-step loss function in Theorem 2.3, and take the associated pretraining domain to be $D_0^{(k)}$. By assumption, the regularity and coverage conditions required by Theorem 2.3 hold for this step- k instantiation, hence the conclusion of Theorem 2.3 yields constants $C_k \geq 1$ and $L_{(k)} \geq 0$ such that

$$\ell_{\text{ICL}}^k(\mathbf{z}) \leq C_k \exp(L_{(k)}^2) \cdot \sup_{\mathbf{z}' \in D_0^{(k)}} \ell_{\text{ICL}}^k(\mathbf{z}'), \quad \forall \mathbf{z} \notin D_0^{(k)}.$$

Evaluating this inequality at $\mathbf{z} = \mathbf{z}^{(k)}$ gives the desired result. \square

E.2 Proof of Theorem E.5

We first present a more general version of the theorem.

Theorem E.5 (ICL Generalization Bound with CoT Prompting, formal version of Theorem 3.1).
Under Assumptions E.1–E.3,

$$\ell_{ICL}(\mathbf{z}^{(K-1)}) \leq R_{K-1} + L_{K-1}^* \sum_{m=0}^{K-2} \left(\prod_{j=m+1}^{K-2} \alpha_j \right) \beta_m \ell_{ICL}(\mathbf{z}^{(m)}), \quad (6)$$

where $R_{K-1} := |M(\mathbf{z}^{(K-1)}) - M_*(\mathbf{z}^{*(K-1)})|$.

Substituting the per-step generalization bound yields

$$\ell_{ICL}(\mathbf{z}^{(K-1)}) \leq R_{K-1} + L_{K-1}^* \sum_{m=0}^{K-2} \left(\prod_{j=m+1}^{K-2} \alpha_j \right) \beta_m C_m e^{L^2(m)} \sup_{\mathbf{z}' \in D_0^{(m)}} \ell_{ICL}(\mathbf{z}'). \quad (7)$$

We now proceed with the proof.

Proof. Fix $k \in \{0, \dots, K-2\}$. By Assumption E.2,

$$\Delta_{k+1} \leq \beta_k \ell_{ICL}(\mathbf{z}^{(k)}) + \alpha_k \Delta_k.$$

Iterating from $\Delta_0 = 0$ yields

$$\Delta_{K-1} \leq \sum_{m=0}^{K-2} \left(\prod_{j=m+1}^{K-2} \alpha_j \right) \beta_m \ell_{ICL}(\mathbf{z}^{(m)}).$$

By the triangle inequality,

$$\begin{aligned} \ell_{ICL}(\mathbf{z}^{(K-1)}) &= |M(\mathbf{z}^{(K-1)}) - M_*(\mathbf{z}^{(K-1)})| \\ &\leq |M(\mathbf{z}^{(K-1)}) - M_*(\mathbf{z}^{*(K-1)})| + |M_*(\mathbf{z}^{*(K-1)}) - M_*(\mathbf{z}^{(K-1)})|. \end{aligned}$$

By Assumption E.3, since $\mathbf{z}^{(K-1)}$ and $\mathbf{z}^{*(K-1)}$ are rollout states at step $K-1$ and hence belong to \mathcal{R}_{K-1} , the second term satisfies

$$|M_*(\mathbf{z}^{*(K-1)}) - M_*(\mathbf{z}^{(K-1)})| \leq L_{K-1}^* \Delta_{K-1}.$$

Substituting the bound on Δ_{K-1} gives

$$\ell_{ICL}(\mathbf{z}^{(K-1)}) \leq R_{K-1} + L_{K-1}^* \sum_{m=0}^{K-2} \left(\prod_{j=m+1}^{K-2} \alpha_j \right) \beta_m \ell_{ICL}(\mathbf{z}^{(m)}),$$

which is precisely (6).

Next, by Lemma E.4, for each m we have

$$\ell_{ICL}(\mathbf{z}^{(m)}) \leq C_m e^{L^2(m)} \sup_{\mathbf{z}' \in D_0^{(m)}} \ell_{ICL}(\mathbf{z}').$$

Substituting this inequality term-by-term into the above sum gives (7). This completes the proof. \square

E.3 Models can ignore irrelevant steps in CoT

To empirically verify that language models can effectively ignore irrelevant steps in a CoT prompt, we examine whether this suppression capability is acquired during pretraining rather than imposed by the prompting format.

Setup. We consider the arithmetic addition task. We pretrain a Llama3.2-3B model on addition while injecting varying proportions of Shakespearean text into the pretraining corpus as structured distractors, where Shakespeare-less, Shakespeare-mid, and Shakespeare-more denote mixing ratios of 0%, 20%, and 50% Shakespearean content, respectively. During training, the model is instructed to perform the addition specified by the prompt (here we use the *In-distribution decomposition* CoT chain provided in Appendix H.4), while the surrounding Shakespearean passages are entirely irrelevant to the target computation. If the model can still learn the intended input-output mapping despite substantial task-irrelevant content, it must have developed the capacity to selectively ignore such distractors. We evaluate model accuracy on held-out addition prompts across different distractor ratios.

Results. As shown in Figure 2, even with a substantial proportion of Shakespearean text included during pretraining, the model achieves strong performance on the addition task when prompted with CoT. While accuracy degrades slightly as distractor content increases, the model remains capable of effectively suppressing irrelevant information and focusing on the core arithmetic operation. This supports our theoretical claim in Theorem 3.1 that language models can learn to ignore irrelevant CoT steps, enabling robust generalization even under significant distraction.

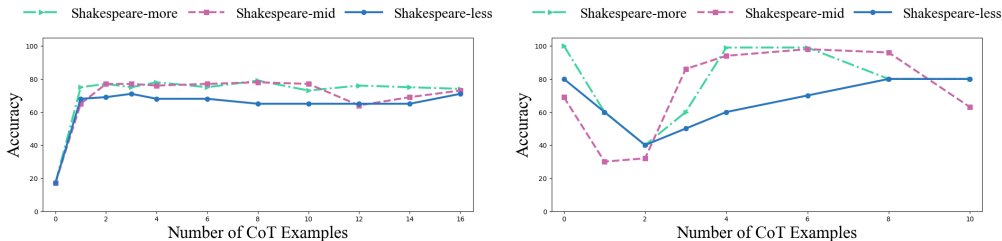


Figure 2: **Effect of structured distractors introduced during pretraining on CoT performance.** Shakespeare less/mid/more denote progressively larger proportions of Shakespearean corpus mixed into the pretraining data. At evaluation time, the model is prompted to solve addition problems using CoT. Despite substantial irrelevant context, the model retains strong CoT performance at inference, indicating an ability to suppress task-irrelevant information.

F Proof of Theorem 4.3, Corollary 4.4 and 4.5

F.1 Preliminaries

We begin by expanding the posterior distribution over tasks using Bayes’ rule. For any task $t \in \mathcal{T}$, conditioning on the full prompt $\mathbf{z} = (\mathbf{i}, \{(x_n, y_n)\}_{n=1}^N, x_{\text{query}})$ yields

$$p(t | \mathbf{z}) = \frac{\pi(t) p(\mathbf{z} | t)}{\sum_{s \in \mathcal{T}} \pi(s) p(\mathbf{z} | s)}. \tag{8}$$

Under prompt formats 1–5, the likelihood $p(\mathbf{z} | t)$ factorizes as

$$p(\mathbf{z} | t) = p(\mathbf{i} | t) p(x_{\text{query}} | t) \prod_{n=1}^N p(x_n, y_n | t), \quad (9)$$

where the instruction, query input, and demonstration pairs are conditionally independent given the latent task t .

Substituting (9) into (8), we obtain

$$p(t | \mathbf{z}) = \frac{\pi(t) p(\mathbf{i} | t) p(x_{\text{query}} | t) \prod_{n=1}^N p(x_n, y_n | t)}{\sum_{s \in \mathcal{T}} \pi(s) p(\mathbf{i} | s) p(x_{\text{query}} | s) \prod_{n=1}^N p(x_n, y_n | s)}.$$

To make the dependence on the number of demonstrations explicit, we compare each task t against the true task t^* by forming posterior odds. For any $t \neq t^*$, dividing $p(t | \mathbf{z})$ by $p(t^* | \mathbf{z})$ gives

$$\frac{p(t | \mathbf{z})}{p(t^* | \mathbf{z})} = \frac{\pi(t)}{\pi(t^*)} \cdot \frac{p(\mathbf{i} | t)}{p(\mathbf{i} | t^*)} \cdot \frac{p(x_{\text{query}} | t)}{p(x_{\text{query}} | t^*)} \cdot \frac{\prod_{n=1}^N p(x_n, y_n | t)}{\prod_{n=1}^N p(x_n, y_n | t^*)}.$$

For notational convenience, we separate the contribution of the demonstrations from all remaining factors. Specifically, we define the *task likelihood ratio induced by demonstrations*

$$B_t := \frac{\prod_{n=1}^N p(x_n, y_n | t)}{\prod_{n=1}^N p(x_n, y_n | t^*)},$$

and the *non-demonstration ratio* (prior, instruction, and query input)

$$A_t(\mathbf{i}) := \frac{\pi(t)}{\pi(t^*)} \cdot \frac{p(\mathbf{i} | t)}{p(\mathbf{i} | t^*)} \cdot \frac{p(x_{\text{query}} | t)}{p(x_{\text{query}} | t^*)}.$$

With these definitions, the posterior odds admit the compact form

$$\frac{p(t | \mathbf{z})}{p(t^* | \mathbf{z})} = A_t(\mathbf{i}) B_t, \quad t \neq t^*.$$

Using the normalization condition $\sum_{t \in \mathcal{T}} p(t | \mathbf{z}) = 1$, the posterior distribution can equivalently be written as

$$p(t^* | \mathbf{z}) = \frac{1}{1 + \sum_{s \neq t^*} A_s(\mathbf{i}) B_s}, \quad p(t | \mathbf{z}) = \frac{A_t(\mathbf{i}) B_t}{1 + \sum_{s \neq t^*} A_s(\mathbf{i}) B_s}, \quad t \neq t^*. \quad (10)$$

Then we present two lemmas.

Lemma F.1 (Exponential Decay of Demonstration Likelihood Ratio). *Defining*

$$\alpha := \frac{1}{2} \min_{t \neq t^*} \kappa_t > 0,$$

there exists $N_0 < \infty$ such that almost surely, for all $N \geq N_0$ and all $t \neq t^$,*

$$B_t \leq e^{-\alpha N}.$$

Proof. Fix any $t \neq t^*$. By the strong law of large numbers and Assumption 4.1,

$$\frac{1}{N} \sum_{n=1}^N \log \frac{p(x_n, y_n | t)}{p(x_n, y_n | t^*)} \xrightarrow{\text{a.s.}} -\text{KL}\left(P_{x,y|t^*} \| P_{x,y|t}\right) =: -\kappa_t,$$

where $\kappa_t > 0$. Hence, almost surely, there exists $N_t < \infty$ such that for all $N \geq N_t$,

$$B_t \leq \exp\left(-(\kappa_t/2)N\right).$$

Since \mathcal{T} is finite, letting

$$\alpha := \frac{1}{2} \min_{t \neq t^*} \kappa_t > 0,$$

we have (after enlarging $N_0 := \max_{t \neq t^*} N_t$) that almost surely, for all $N \geq N_0$ and all $t \neq t^*$,

$$B_t \leq e^{-\alpha N}.$$

□

Lemma F.2 (Uniform Boundedness of Non-Demonstration Ratio). *There exists a finite constant A_{\max} such that*

$$\sup_{i \in D} \max_{t \neq t^*} A_t(\mathbf{i}) \leq A_{\max} < \infty.$$

Proof. Recall that

$$A_t(\mathbf{i}) = \frac{\pi(t)}{\pi(t^*)} \cdot \frac{p(\mathbf{i} | t)}{p(\mathbf{i} | t^*)} \cdot \frac{p(x_{\text{query}} | t)}{p(x_{\text{query}} | t^*)}.$$

Since \mathcal{T} is finite and x_{query} is fixed, the quantities $\max_{t \neq t^*} \frac{\pi(t)}{\pi(t^*)}$ and $\max_{t \neq t^*} \frac{p(x_{\text{query}} | t)}{p(x_{\text{query}} | t^*)}$ are finite constants. Thus it suffices to show that

$$\sup_{i \in D} \max_{t \neq t^*} \frac{p(\mathbf{i} | t)}{p(\mathbf{i} | t^*)} < \infty.$$

By Assumption 4.2, there exists $G < \infty$ such that for all $t \in \mathcal{T}$ and all $\mathbf{i} \in D$,

$$\|\nabla_{\mathbf{i}} \log p(\mathbf{i} | t)\|_2 \leq G.$$

Fix an arbitrary reference instruction $\mathbf{i}_0 \in D$. For any $\mathbf{i} \in D$ and any $t \in \mathcal{T}$, by the mean value theorem applied to the differentiable function $\log p(\cdot | t)$ along the line segment between \mathbf{i}_0 and \mathbf{i} ,

$$\left| \log p(\mathbf{i} | t) - \log p(\mathbf{i}_0 | t) \right| \leq \sup_{\tilde{\mathbf{i}} \in [\mathbf{i}_0, \mathbf{i}]} \|\nabla_{\mathbf{i}} \log p(\tilde{\mathbf{i}} | t)\|_2 \cdot \|\mathbf{i} - \mathbf{i}_0\|_2 \leq G \|\mathbf{i} - \mathbf{i}_0\|_2.$$

Since D is bounded (compact), its diameter is finite:

$$D := \sup_{\mathbf{i} \in D} \|\mathbf{i} - \mathbf{i}_0\|_2 < \infty.$$

Hence for all $\mathbf{i} \in D$ and all $t \in \mathcal{T}$,

$$\log p(\mathbf{i} | t) \leq \log p(\mathbf{i}_0 | t) + GD, \quad \log p(\mathbf{i} | t) \geq \log p(\mathbf{i}_0 | t) - GD.$$

Applying the same bounds to t^* and subtracting gives, for all $\mathbf{i} \in D$ and all $t \in \mathcal{T}$,

$$\log \frac{p(\mathbf{i} | t)}{p(\mathbf{i} | t^*)} = \log p(\mathbf{i} | t) - \log p(\mathbf{i} | t^*) \leq (\log p(\mathbf{i}_0 | t) - \log p(\mathbf{i}_0 | t^*)) + 2GD.$$

Exponentiating and taking maxima over the finite task set yields

$$\sup_{\mathbf{i} \in D} \max_{t \neq t^*} \frac{p(\mathbf{i} | t)}{p(\mathbf{i} | t^*)} \leq \left(\max_{t \neq t^*} \frac{p(\mathbf{i}_0 | t)}{p(\mathbf{i}_0 | t^*)} \right) e^{2GD} < \infty,$$

where finiteness holds because \mathcal{T} is finite and $p(\mathbf{i}_0 | t) > 0$ on the support of the instruction domain.

Combining with the finite constants $\max_{t \neq t^*} \frac{\pi(t)}{\pi(t^*)}$ and $\max_{t \neq t^*} \frac{p(x_{\text{query}} | t)}{p(x_{\text{query}} | t^*)}$ gives the desired bound with

$$A_{\max} := \left(\max_{t \neq t^*} \frac{\pi(t)}{\pi(t^*)} \right) \left(\max_{t \neq t^*} \frac{p(x_{\text{query}} | t)}{p(x_{\text{query}} | t^*)} \right) \left(\max_{t \neq t^*} \frac{p(\mathbf{i}_0 | t)}{p(\mathbf{i}_0 | t^*)} \right) e^{2GD}.$$

□

F.2 Proof of Theorem 4.3

We first recall the statement of the theorem for convenience.

Theorem F.3 (Exponential Convergence of Posterior Predictive (Formats 1–5)). *Consider prompt formats 1–5. Under Assumptions 4.1 and 4.2, there exist constants $\alpha, \beta > 0$ such that, with high probability, for all sufficiently large numbers of demonstrations N ,*

$$|p(y_{\text{query}} | \mathbf{z}) - p(y_{\text{query}} | x_{\text{query}}, t^*)| \leq \beta \exp(-\alpha N).$$

Equivalently, for any two instructions \mathbf{i}, \mathbf{i}' (with all non-instruction parts of \mathbf{z} fixed), we have

$$|p(y_{\text{query}} | \mathbf{z}(\mathbf{i})) - p(y_{\text{query}} | \mathbf{z}(\mathbf{i}'))| \leq 2\beta \exp(-\alpha N).$$

We now proceed with the proof.

Proof. By definition of the posterior predictive,

$$p(y_{\text{query}} | \mathbf{z}) = \sum_{t \in \mathcal{T}} p(y_{\text{query}} | x_{\text{query}}, t) p(t | \mathbf{z}). \quad (11)$$

Subtracting $p(y_{\text{query}} | x_{\text{query}}, t^*)$ and using $\sum_t p(t | \mathbf{z}) = 1$ yields

$$p(y_{\text{query}} | \mathbf{z}) - p(y_{\text{query}} | x_{\text{query}}, t^*) = \sum_{t \neq t^*} (p(y_{\text{query}} | x_{\text{query}}, t) - p(y_{\text{query}} | x_{\text{query}}, t^*)) p(t | \mathbf{z}).$$

Since $0 \leq p(y_{\text{query}} | x_{\text{query}}, t) \leq 1$, we have $|p(y_{\text{query}} | x_{\text{query}}, t) - p(y_{\text{query}} | x_{\text{query}}, t^*)| \leq 1$ for all t , hence

$$|p(y_{\text{query}} | \mathbf{z}) - p(y_{\text{query}} | x_{\text{query}}, t^*)| \leq \sum_{t \neq t^*} p(t | \mathbf{z}). \quad (12)$$

It remains to upper bound the posterior mass on wrong tasks. From Equation (10), for any $t \neq t^*$,

$$p(t | \mathbf{z}) = \frac{A_t(\mathbf{i})B_t}{1 + \sum_{s \neq t^*} A_s(\mathbf{i})B_s} \leq A_t(\mathbf{i})B_t.$$

Summing over $t \neq t^*$ and applying Lemma F.1 and F.2, we obtain that almost surely for all $N \geq N_0$,

$$\sum_{t \neq t^*} p(t | \mathbf{z}) \leq \sum_{t \neq t^*} A_t(\mathbf{i})B_t \leq (|\mathcal{T}| - 1) A_{\max} e^{-\alpha N}. \quad (13)$$

Combining Equations (12) and (13) proves the first statement with $\beta := (|\mathcal{T}| - 1)A_{\max}$:

$$|p(y_{\text{query}} | \mathbf{z}) - p(y_{\text{query}} | x_{\text{query}}, t^*)| \leq \beta e^{-\alpha N}.$$

For the equivalent statement comparing two instructions \mathbf{i}, \mathbf{i}' (with all other parts of \mathbf{z} fixed), we use the triangle inequality:

$$\begin{aligned} & |p(y_{\text{query}} | \mathbf{z}(\mathbf{i})) - p(y_{\text{query}} | \mathbf{z}(\mathbf{i}'))| \\ & \leq |p(y_{\text{query}} | \mathbf{z}(\mathbf{i})) - p(y_{\text{query}} | x_{\text{query}}, t^*)| + |p(y_{\text{query}} | \mathbf{z}(\mathbf{i}')) - p(y_{\text{query}} | x_{\text{query}}, t^*)| \\ & \leq 2\beta e^{-\alpha N}, \end{aligned}$$

which completes the proof. \square

F.3 Proof of Corollary 4.4

We first recall the statement of the corollary for convenience.

Corollary F.4 (Gradient Decay of Prompt Sensitivity). *Under the conditions of Theorem 4.3, then there exist constants $\alpha', \beta' > 0$ such that, with high probability, for all sufficiently large N ,*

$$\|\nabla_{\mathbf{i}} p(y_{\text{query}} | \mathbf{z})\| \leq \beta' \exp(-\alpha' N).$$

We now proceed with the proof.

Proof. We start from Equation (11). Since $p(y_{\text{query}} | x_{\text{query}}, t)$ is independent of \mathbf{i} under formats 1–5, differentiating gives

$$\nabla_{\mathbf{i}} p(y_{\text{query}} | \mathbf{z}) = \sum_{t \in \mathcal{T}} p(y_{\text{query}} | x_{\text{query}}, t) \nabla_{\mathbf{i}} p(t | \mathbf{z}),$$

hence by $0 \leq p(y_{\text{query}} | x_{\text{query}}, t) \leq 1$ and the triangle inequality,

$$\|\nabla_{\mathbf{i}} p(y_{\text{query}} | \mathbf{z})\| \leq \sum_{t \in \mathcal{T}} \|\nabla_{\mathbf{i}} p(t | \mathbf{z})\|. \quad (14)$$

Next we control $\|\nabla_{\mathbf{i}} p(t | \mathbf{z})\|$. Differentiating the softmax-form posterior yields the standard identity

$$\nabla_{\mathbf{i}} p(t | \mathbf{z}) = p(t | \mathbf{z}) \left(\nabla_{\mathbf{i}} \log p(\mathbf{i} | t) - \sum_{s \in \mathcal{T}} p(s | \mathbf{z}) \nabla_{\mathbf{i}} \log p(\mathbf{i} | s) \right).$$

By Assumption 4.2, $\|\nabla_{\mathbf{i}} \log p(\mathbf{i} | t)\| \leq G$ for all t , thus

$$\|\nabla_{\mathbf{i}} p(t | \mathbf{z})\| \leq p(t | \mathbf{z}) \left(G + \sum_{s \in \mathcal{T}} p(s | \mathbf{z}) G \right) \leq 2G p(t | \mathbf{z}). \quad (15)$$

Now we sum over t . Use $\sum_{t \in \mathcal{T}} p(t | \mathbf{z}) = 1$ to relate the gradient of the true task to the others:

$$\nabla_{\mathbf{i}} p(t^* | \mathbf{z}) = - \sum_{t \neq t^*} \nabla_{\mathbf{i}} p(t | \mathbf{z}), \quad \Rightarrow \quad \|\nabla_{\mathbf{i}} p(t^* | \mathbf{z})\| \leq \sum_{t \neq t^*} \|\nabla_{\mathbf{i}} p(t | \mathbf{z})\|.$$

Therefore,

$$\sum_{t \in \mathcal{T}} \|\nabla_{\mathbf{i}} p(t | \mathbf{z})\| \leq 2 \sum_{t \neq t^*} \|\nabla_{\mathbf{i}} p(t | \mathbf{z})\| \stackrel{(15)}{\leq} 4G \sum_{t \neq t^*} p(t | \mathbf{z}). \quad (16)$$

Finally, by Equation (13) (proved in the theorem proof), almost surely for all $N \geq N_0$,

$$\sum_{t \neq t^*} p(t \mid \mathbf{z}) \leq (|\mathcal{T}| - 1) A_{\max} e^{-\alpha N}.$$

Combining with Equations (14) and (16) gives

$$\|\nabla_{\mathbf{z}} p(y_{\text{query}} \mid \mathbf{z})\| \leq 4G(|\mathcal{T}| - 1) A_{\max} e^{-\alpha N}.$$

Thus the corollary holds with $\alpha' = \alpha$ and $\beta' = 4G(|\mathcal{T}| - 1) A_{\max}$. \square

F.4 Proof of Corollary 4.5

We first introduce the notation used in this proof and make an essential realizability assumption.

Assumption F.5 (Log-space realizability and positivity). There exists $\delta > 0$ such that

$$q^*(\mathbf{z}) \geq \delta \quad \text{for all } \mathbf{z} \text{ in the support of } \mu_N, \quad (17)$$

and for any $\epsilon > 0$, there exists a parameter θ_0 in the considered model class such that

$$\sup_{\mathbf{z} \text{ in the support of } \mu_N} |\log q_{\theta_0}(\mathbf{z}) - \log q^*(\mathbf{z})| \leq \epsilon.$$

Moreover, the trained predictor is bounded away from zero on the same support: for the parameter $\hat{\theta}$ returned by training (defined below),

$$q_{\hat{\theta}}(\mathbf{z}) \geq \delta \quad \text{for all } \mathbf{z} \text{ in the support of } \mu_N. \quad (18)$$

Assumption F.5 is aligned with the cross-entropy training objective, which minimizes the (log-space) risk $\mathbb{E}_{\mathbf{z} \sim \mu_N} [-\log q_{\theta}(\mathbf{z})]$. Hence, realizability in log-space is the natural notion of approximation for predictors learned by cross-entropy training. The lower bound (17) avoids singularities of the log-loss, and (18) ensures that log-space control can be converted into control in probability space.

We now proceed with the proof.

Proof. Fix a demonstration count N and let μ_N be the distribution over prompts of formats 1–5 with exactly N demonstrations (with the non-instruction parts fixed). Write $q^*(\mathbf{z}) := p(y_{\text{query}} \mid \mathbf{z})$ for the Bayesian predictor and $q_{\theta}(\mathbf{z}) := p_{\theta}(y_{\text{query}} \mid \mathbf{z})$ for the transformer predictor.

Let $\hat{\theta}$ be the parameter obtained by (approximately) minimizing the cross-entropy objective over the same prompt distribution μ_N :

$$\hat{\theta} \in \arg \min_{\theta} \mathbb{E}_{\mathbf{z} \sim \mu_N} [-\log q_{\theta}(\mathbf{z})].$$

By definition of risk minimization, the trained solution is not worse than the candidate θ_0 : there exists $\eta_{\text{train}} \geq 0$ capturing optimization and statistical error such that

$$\mathbb{E}_{\mathbf{z} \sim \mu_N} [-\log q_{\hat{\theta}}(\mathbf{z})] \leq \mathbb{E}_{\mathbf{z} \sim \mu_N} [-\log q_{\theta_0}(\mathbf{z})] + \eta_{\text{train}}.$$

Define the *log-space approximation error in expectation*

$$\epsilon_N^{\log} := \mathbb{E}_{\mathbf{z} \sim \mu_N} \left[\left| \log q_{\hat{\theta}}(\mathbf{z}) - \log q^*(\mathbf{z}) \right| \right].$$

We treat ε_N^{\log} as the pretraining/training error term induced by cross-entropy training (on μ_N), and note that it is expected to decrease as the model class becomes more expressive and optimization/statistical errors shrink. (The subsequent bound is stated in terms of ε_N^{\log} and does not require identifying its exact dependence on architecture size.)

From log-space error to probability-space error. For any $a, b \in [\delta, 1]$, the mean value theorem applied to $\exp(\cdot)$ gives

$$|a - b| = |e^{\log a} - e^{\log b}| = e^\xi |\log a - \log b| \leq |\log a - \log b|,$$

for some ξ between $\log a$ and $\log b$, where we used $e^\xi \leq 1$ since $\xi \leq 0$. Applying this inequality with $a = q_{\hat{\theta}}(\mathbf{z})$ and $b = q^*(\mathbf{z})$ (which lie in $[\delta, 1]$ by (17) and (18)) and taking expectations yields

$$\mathbb{E}_{\mathbf{z} \sim \mu_N} \left[|q_{\hat{\theta}}(\mathbf{z}) - q^*(\mathbf{z})| \right] \leq \varepsilon_N^{\log}.$$

Letting

$$\varepsilon_N := \mathbb{E}_{\mathbf{z} \sim \mu_N} \left[|q_{\hat{\theta}}(\mathbf{z}) - q^*(\mathbf{z})| \right],$$

we obtain $\varepsilon_N \leq \varepsilon_N^{\log}$.

Conclude by triangle inequality. Using the triangle inequality exactly as in the proof strategy for the instruction-decay bound,

$$\begin{aligned} \mathbb{E}_{\mathbf{z} \sim \mu_N} \left[|q_{\hat{\theta}}(\mathbf{z}(\mathbf{i})) - q_{\hat{\theta}}(\mathbf{z}(\mathbf{i}'))| \right] &\leq \mathbb{E}_{\mathbf{z} \sim \mu_N} \left[|q_{\hat{\theta}}(\mathbf{z}(\mathbf{i})) - q^*(\mathbf{z}(\mathbf{i}))| \right] + \mathbb{E}_{\mathbf{z} \sim \mu_N} \left[|q^*(\mathbf{z}(\mathbf{i})) - q^*(\mathbf{z}(\mathbf{i}'))| \right] \\ &\quad + \mathbb{E}_{\mathbf{z} \sim \mu_N} \left[|q^*(\mathbf{z}(\mathbf{i}')) - q_{\hat{\theta}}(\mathbf{z}(\mathbf{i}'))| \right]. \end{aligned}$$

By Theorem 4.3 (applied to the Bayes predictor), the middle term is bounded by $2\beta e^{-\alpha N}$. The first and third terms are each bounded by $\mathbb{E}_{\mathbf{z} \sim \mu_N} \left[|q_{\hat{\theta}}(\mathbf{z}) - q^*(\mathbf{z})| \right] = \varepsilon_N$, since only the instruction component varies and the expectation is over the same μ_N with non-instruction parts fixed. Therefore,

$$\mathbb{E}_{\mathbf{z} \sim \mu_N} \left[|q_{\hat{\theta}}(\mathbf{z}(\mathbf{i})) - q_{\hat{\theta}}(\mathbf{z}(\mathbf{i}'))| \right] \leq 2\beta e^{-\alpha N} + 2\varepsilon_N,$$

which is the claimed bound (3). □

G Proof of Theorem 4.7 and Corollary 4.8

In this appendix, we provide a complete proof of the formal Lipschitz generalization bound stated in Section 2. The proof follows the same overall strategy as the proof sketch in the main text: we first restrict the loss to a one-dimensional path connecting the test prompt to the pretraining domain, then approximate the resulting path-restricted loss by a Bernstein polynomial, apply the Remez inequality to transfer control from the pretraining portion of the path to the full path, and finally optimize the polynomial degree to obtain the stated bound. We restate Theorem 4.7 in a fully explicit form. Throughout this appendix, we work under prompt format 6, in which each demonstration is associated with its own instruction, and we consider the instruction *sequence* as the variable.

The instruction is a length- N sequence whose embedding is denoted by $I \in \mathbb{R}^k$ with $k = Nd$.

$$I^{\text{inner}} := (i^*, \dots, i^*) \in \mathbb{R}^k, \quad D_{i_0} := B_r(I^{\text{inner}}), \quad D_i := B_R(I^{\text{inner}}).$$

Theorem G.1 (Failure of convergence of posterior predictive (Format 6), formal version of Theorem 4.7). *Consider prompt format 6, under Assumptions 4.1 and 4.2, and fix radii $0 < r < R$. Almost surely, there exist constants $\alpha > 0$ and $N_0 < \infty$ such that for all $N \geq N_0$ and all polynomial degrees $n \geq 1$,*

$$\|f - f^*\|_{L^\infty(D_i)} \leq \exp(C_1 kn) \left(\beta(N) e^{-\alpha N} + \varepsilon_n \right) + \varepsilon_n, \quad (19)$$

where $C_1 = \log(2R/r)$, $\beta(N) := (|\mathcal{T}| - 1)A_{\max}(N)$ with $A_{\max}(N) = O(e^{2G\sqrt{N}r})$ depending on N , and

$$\varepsilon_n \leq c_0 GR \sqrt{d} \frac{N}{\sqrt{n}}, \quad (20)$$

with an absolute constant $c_0 > 0$.

G.1 Preliminaries

We follow the Bayesian decomposition used in Theorem 4.3, and then show how the high-dimensional instruction variable in format 6 prevents extending inner-region control to the outer region.

Posterior predictive decomposition. By definition,

$$f(I) = p(y_{\text{query}} | \mathbf{z}(I)) = \sum_{t \in \mathcal{T}} p(y_{\text{query}} | x_{\text{query}}, t) p(t | \mathbf{z}(I)).$$

Since $p(y_{\text{query}} | x_{\text{query}}, t)$ does not depend on I under format 6, subtracting $f^* = p(y_{\text{query}} | x_{\text{query}}, t^*)$ and using $\sum_t p(t | \mathbf{z}) = 1$ gives

$$|f(I) - f^*| = \left| \sum_{t \neq t^*} (p(y_{\text{query}} | x_{\text{query}}, t) - p(y_{\text{query}} | x_{\text{query}}, t^*)) p(t | \mathbf{z}(I)) \right| \leq \sum_{t \neq t^*} p(t | \mathbf{z}(I)). \quad (21)$$

Thus it suffices to upper bound the posterior mass on wrong tasks.

Posterior odds and task concentration (inner region). Bayes' rule yields, for each $t \in \mathcal{T}$,

$$p(t | \mathbf{z}(I)) \propto \pi(t) p(I | t) p(x_{\text{query}} | t) \prod_{n=1}^N p(x_n, y_n | t).$$

Fix $t \neq t^*$. Forming posterior odds against t^* as in Theorem 4.3 gives

$$\frac{p(t | \mathbf{z}(I))}{p(t^* | \mathbf{z}(I))} = \underbrace{\frac{\pi(t)}{\pi(t^*)} \cdot \frac{p(I | t)}{p(I | t^*)} \cdot \frac{p(x_{\text{query}} | t)}{p(x_{\text{query}} | t^*)}}_{=: A_t(I)} \cdot \underbrace{\frac{\prod_{n=1}^N p(x_n, y_n | t)}{\prod_{n=1}^N p(x_n, y_n | t^*)}}_{=: B_t}. \quad (22)$$

By Assumption 4.1 and the strong law of large numbers (exactly the same argument as in Theorem 4.3), almost surely there exist $\alpha > 0$ and $N_0 < \infty$ such that for all $N \geq N_0$ and all $t \neq t^*$,

$$B_t \leq e^{-\alpha N}. \quad (23)$$

It remains to control $A_t(I)$ on the inner ball $D_{i_0} = B_r(I^{\text{inner}})$. Since each demonstration carries its own instruction, the joint instruction likelihood factorizes as $p(I | t) = \prod_{n=1}^N p(i_n | t)$, so

$\log p(I | t) = \sum_{n=1}^N \log p(i_n | t)$. By Assumption 4.2, $\|\nabla_{i_n} \log p(i_n | t)\|_2 \leq G$ for every n and t , hence

$$\|\nabla_I \log p(I | t)\|_2 = \sqrt{\sum_{n=1}^N \|\nabla_{i_n} \log p(i_n | t)\|_2^2} \leq G\sqrt{N}.$$

Thus $\log p(I | t)$ is $G\sqrt{N}$ -Lipschitz on \mathbb{R}^k . For any $I \in D_{i_0}$, applying the mean value theorem to both t and t^* and subtracting gives

$$\left| \log \frac{p(I | t)}{p(I | t^*)} - \log \frac{p(I^{\text{inner}} | t)}{p(I^{\text{inner}} | t^*)} \right| \leq 2G\sqrt{N} \|I - I^{\text{inner}}\|_2 \leq 2G\sqrt{N} r.$$

Exponentiating,

$$\sup_{I \in D_{i_0}} \frac{p(I | t)}{p(I | t^*)} \leq e^{2G\sqrt{N}r} \cdot \frac{p(I^{\text{inner}} | t)}{p(I^{\text{inner}} | t^*)}.$$

Therefore $\sup_{I \in D_{i_0}} A_t(I)$ is finite for each t and N , and since \mathcal{T} is finite we may define

$$A_{\max}(N) := \max_{t \neq t^*} \sup_{I \in D_{i_0}} A_t(I) = O\left(e^{2G\sqrt{N}r}\right).$$

Combining (22)–(23) and using $p(t | z) \leq A_t(I)B_t$ (since the posterior denominator is at least 1), we obtain that almost surely, for all $N \geq N_0$ and all $I \in D_{i_0}$,

$$\sum_{t \neq t^*} p(t | z(I)) \leq \sum_{t \neq t^*} A_t(I)B_t \leq (|\mathcal{T}| - 1) A_{\max}(N) e^{-\alpha N}. \quad (24)$$

Plugging (24) into (21) yields the inner-region bound:

$$\|f - f^*\|_{L^\infty(D_{i_0})} \leq \beta(N) e^{-\alpha N}, \quad \beta(N) := (|\mathcal{T}| - 1) A_{\max}(N). \quad (25)$$

Note that $\beta(N) = O(e^{2G\sqrt{N}r})$ grows with N , so the inner-region bound itself does not imply convergence as $N \rightarrow \infty$.

Multivariate Bernstein approximation on a bounding cube. To define a polynomial approximation over D_i , we embed the ball $D_i = B_R(I^{\text{inner}})$ into the bounding cube $Q := I^{\text{inner}} + [-R, R]^k$. We map Q affinely onto the unit cube $[0, 1]^k$ via the bijection $\Phi(I)_j$ and consider the pullback $h := (f - f^*) \circ \Phi^{-1}$ on $[0, 1]^k$.

For an integer parameter $n \geq 1$, the k -variate Bernstein polynomial (tensor product of 1D Bernstein polynomials) is defined by

$$(B_n^{(k)} h)(x) := \sum_{j_1=0}^n \cdots \sum_{j_k=0}^n h\left(\frac{j_1}{n}, \dots, \frac{j_k}{n}\right) \prod_{\ell=1}^k \binom{n}{j_\ell} x_\ell^{j_\ell} (1 - x_\ell)^{n-j_\ell}, \quad x \in [0, 1]^k. \quad (26)$$

Let $p_n := B_n^{(k)} h$ (identified with a function on Q via Φ). Note that the highest monomial in (26) is $\prod_{\ell=1}^k x_\ell^n$, so p_n has a *total degree* of nk .

The coefficients in (26) form a convex combination, so the Bernstein polynomial at x equals the expectation of h at the random grid point S/n , where $S = (S_1, \dots, S_k)$ with $S_j \sim \text{Binomial}(n, x_j)$ independently:

$$(B_n^{(k)} h)(x) = \mathbb{E} \left[h \left(\frac{S}{n} \right) \right].$$

Assuming h is Lipschitz with constant L_h (determined below), Jensen's inequality yields

$$|(B_n^{(k)}h)(x) - h(x)| \leq L_h \mathbb{E} \left\| \frac{S}{n} - x \right\| \leq L_h \sqrt{\mathbb{E} \left\| \frac{S}{n} - x \right\|^2}.$$

Since $\text{Var}(S_j/n) = x_j(1-x_j)/n \leq 1/(4n)$ and the coordinates are independent,

$$\mathbb{E} \left\| \frac{S}{n} - x \right\|^2 = \sum_{j=1}^k \text{Var} \left(\frac{S_j}{n} \right) \leq \frac{k}{4n}.$$

Hence, bounding the error over the cube Q (and thereby over the inscribed ball D_i), we have

$$\varepsilon_n := \|p_n - h\|_{L^\infty([0,1]^k)} \leq L_h \sqrt{\frac{k}{4n}}.$$

G.2 Proof of Theorem 4.7

Proof. Under format 6, $I = (i_1, \dots, i_N) \in \mathbb{R}^k$ is a concatenation of N per-demonstration instruction embeddings $i_n \in \mathbb{R}^d$, with $k = Nd$. Using the factorization $\log p(I | t) = \sum_{n=1}^N \log p(i_n | t)$ established above, differentiating with respect to the n -th block gives $\nabla_{i_n} \log p(I | t) = \nabla_{i_n} \log p(i_n | t)$, and Assumption 4.2 yields $\|\nabla_{i_n} \log p(I | t)\|_2 \leq G$ for all n and t . The softmax-gradient identity applied to each block gives

$$\nabla_{i_n} p(t | \mathbf{z}) = p(t | \mathbf{z}) \left(\nabla_{i_n} \log p(I | t) - \sum_{s \in \mathcal{T}} p(s | \mathbf{z}) \nabla_{i_n} \log p(I | s) \right),$$

so $\|\nabla_{i_n} p(t | \mathbf{z})\|_2 \leq 2G p(t | \mathbf{z})$. Summing over t ,

$$\|\nabla_{i_n} f(I)\|_2 \leq \sum_{t \in \mathcal{T}} 2G p(t | \mathbf{z}(I)) = 2G \quad \text{for each } n.$$

Since the N coordinate blocks are orthogonal directions in \mathbb{R}^k ,

$$\|\nabla_I f(I)\|_2 = \sqrt{\sum_{n=1}^N \|\nabla_{i_n} f(I)\|_2^2} \leq 2G\sqrt{N}.$$

Hence $f - f^*$ is $2G\sqrt{N}$ -Lipschitz on \mathbb{R}^k . The inverse map $\Phi^{-1}(x) = I^{\text{inner}} + 2R(x - \frac{1}{2})$ has a Lipschitz constant of $2R$. Thus, its pullback $h = (f - f^*) \circ \Phi^{-1}$ is Lipschitz with constant $L_h = 4RG\sqrt{N}$. Substituting into the Bernstein error bound gives

$$\varepsilon_n \leq 4RG\sqrt{N} \cdot \sqrt{\frac{Nd}{4n}} = c_0 GR\sqrt{d} \cdot \frac{N}{\sqrt{n}},$$

where $c_0 = 2$, yielding (20).

On the inner ball D_{i_0} ,

$$\|p_n\|_{L^\infty(D_{i_0})} \leq \|f - f^*\|_{L^\infty(D_{i_0})} + \varepsilon_n \leq \beta(N) e^{-\alpha N} + \varepsilon_n.$$

Recall that p_n is a polynomial of total degree nk . Because D_{i_0} and D_i are concentric balls, the restriction of p_n to any line passing through I^{inner} is a 1D polynomial of degree at most nk . Applying

the standard 1D Chebyshev extremum property to the segments $[-r, r]$ and $[-R, R]$ along any such ray gives

$$\|p_n\|_{L^\infty(D_i)} \leq T_{nk} \left(\frac{R}{r} \right) \|p_n\|_{L^\infty(D_{i_0})},$$

where T_{nk} denotes the Chebyshev polynomial of the first kind of degree nk . Using the bound $T_m(x) \leq (2x)^m$ for $x \geq 1$ yields

$$\|p_n\|_{L^\infty(D_i)} \leq \left(\frac{2R}{r} \right)^{nk} \|p_n\|_{L^\infty(D_{i_0})} = \exp(C_1 kn) \|p_n\|_{L^\infty(D_{i_0})}, \quad C_1 := \log(2R/r).$$

Therefore,

$$\|p_n\|_{L^\infty(D_i)} \leq \exp(C_1 kn) \left(\beta(N) e^{-\alpha N} + \varepsilon_n \right).$$

By the triangle inequality $\|f - f^*\|_{L^\infty(D_i)} \leq \|p_n\|_{L^\infty(D_i)} + \varepsilon_n$, we obtain (19).

Note that $\varepsilon_n = c_0 GR\sqrt{d} \cdot N/\sqrt{n}$ grows with N for any fixed n , and requires $n = \Omega(N^2)$ to remain bounded. However, choosing $n = \Omega(N^2)$ causes the amplification factor to satisfy $\exp(C_1 kn) = \exp(\Omega(dN^3))$, which diverges super-exponentially. Hence no choice of n simultaneously controls both terms, and the bound (19) cannot be made to converge to 0 as $N \rightarrow \infty$. \square

G.3 Proof of Corollary 4.8

To establish stability guarantees on the extended domain D_i , we rely on the following tool.

Lemma G.2 (Multivariate Markov inequality (Wilhelmsen, 1974)). *Let $T \subset \mathbb{R}^k$ be a convex body with diameter w_T , and let $p : \mathbb{R}^k \rightarrow \mathbb{R}$ be a polynomial of total degree at most m . Then*

$$\|\nabla p\|_{L^\infty(T)} \leq \frac{4m^2}{w_T} \|p\|_{L^\infty(T)}.$$

To upper bound $\|\nabla f\|$ on D_i using a polynomial surrogate, uniform C^0 approximation is insufficient in general. We therefore impose a mild C^1 -approximability condition.

Assumption G.3 (Uniform C^1 polynomial approximability on D_i). There exists a polynomial p_n of total degree at most nk such that

$$\|f - p_n\|_{L^\infty(D_i)} \leq \varepsilon_n, \quad \|\nabla f - \nabla p_n\|_{L^\infty(D_i)} \leq \delta_n.$$

Proof. Recall that $D_i = B_R(I^{\text{inner}}) \subset \mathbb{R}^k$ with $k = Nd$, so its diameter is $w_{D_i} = 2R$. Let p_n be the polynomial surrogate of total degree $m = nk$ from Theorem G.3.

By the triangle inequality and the inner-region bound (25),

$$\|p_n\|_{L^\infty(D_{i_0})} \leq \|f - f^*\|_{L^\infty(D_{i_0})} + \|f - p_n\|_{L^\infty(D_{i_0})} \leq \beta(N) e^{-\alpha N} + \varepsilon_n.$$

Since D_{i_0} and D_i are concentric balls, the restriction of p_n to any line through I^{inner} is a one-dimensional polynomial of degree at most nk . Applying the standard Chebyshev growth bound on the concentric intervals $[-r, r]$ and $[-R, R]$ yields

$$\|p_n\|_{L^\infty(D_i)} \leq T_{nk} \left(\frac{R}{r} \right) \|p_n\|_{L^\infty(D_{i_0})},$$

where T_{nk} is the Chebyshev polynomial of the first kind. Using $T_m(x) \leq (2x)^m$ for $x \geq 1$ gives

$$\|p_n\|_{L^\infty(D_i)} \leq \exp(C_1 kn) \left(\beta(N) e^{-\alpha N} + \varepsilon_n \right), \quad C_1 = \log(2R/r). \quad (27)$$

Applying Theorem G.2 with $m = nk$ and $w_{D_i} = 2R$,

$$\|\nabla p_n\|_{L^\infty(D_i)} \leq \frac{4(nk)^2}{2R} \|p_n\|_{L^\infty(D_i)} = \frac{2n^2k^2}{R} \|p_n\|_{L^\infty(D_i)}. \quad (28)$$

Substituting (27) into (28) yields

$$\|\nabla p_n\|_{L^\infty(D_i)} \leq \frac{2n^2k^2}{R} \exp(C_1kn) \left(\beta(N) e^{-\alpha N} + \varepsilon_n \right).$$

Using the C^1 approximation condition and the triangle inequality,

$$\|\nabla f\|_{L^\infty(D_i)} \leq \|\nabla p_n\|_{L^\infty(D_i)} + \delta_n,$$

we obtain

$$\|\nabla f\|_{L^\infty(D_i)} \leq \frac{2n^2k^2}{R} \exp(C_1kn) \left(\beta(N) e^{-\alpha N} + \varepsilon_n \right) + \delta_n.$$

Taking

$$n = \Theta(G^2 R^2 d N^2)$$

controls the Bernstein approximation error $\varepsilon_n = O(1)$ from Theorem G.1. Substituting $k = Nd$ gives the stated scaling. \square

H Experiments

In this section we provide detailed introduction of our experiments setup and additional experimental results to supplement those in the main text.

H.1 Pretraining Dependence

To isolate the role of *intrinsic ICL capability*, we construct three variants of Llama3.2-3B that differ only in the amount and *format* of additional pretraining on a six-digit addition corpus. Throughout, we use the same evaluation protocol in the main text (6–10 digit addition).

Base (Weak). We use the original Llama3.2-3B checkpoint without any additional training.

Fine-tuned (Strong). We randomly generate 20,000 six-digit addition instances and format each instance as a supervised instruction-following sample in JSONL, each training example is serialized as

Instruction: ... Input: ... Response: ...

and we fine-tune the model using LoRA on this dataset.

Fine-tuned (Medium). We use the *same* 20,000 generated instances, but concatenate all serialized training examples into a single long text sequence and fine-tune on this single sequence. This construction preserves the token-level training signal while substantially reducing the effective diversity and sampling of training contexts, leading to a weaker improvement in intrinsic ICL capability compared to the sample-level training above.

Both **Strong** and **Medium** variants are trained with the same LoRA configuration and optimizer settings. We apply LoRA to attention and MLP projection modules. We train a causal LM objective with labels equal to the input tokens (standard next-token prediction over the serialized prompt). Unless otherwise stated, we use a maximum sequence length of 512 tokens with padding/truncation.

H.2 Demonstration Choice

In this section, our goal is to isolate how the informativeness of demonstrations affects in-context generalization, under the same prompt template, the same query distribution, and the same number of demonstrations.

Tasks. We consider two retrieval-style tasks constructed as “ $(x, ?, y)$ ” completion: (i) **Sports**: x is a country and y is its designated sport label in our benchmark; (ii) **People**: x is a company and y is a canonical person name associated with that company in our benchmark (e.g., a founder). The model is queried with an unseen x_{test} and asked to predict the corresponding y_{test} .

Ambiguous vs. identifying demonstration pools. For each task, we build two disjoint pools of demonstration pairs: *ambiguous* and *identifying*. Both pools contain 10 labeled pairs (x, y) . Intuitively, the ambiguous pool contains examples that can be explained by multiple plausible latent rules (hence providing weaker evidence about which rule the prompt instantiates), whereas the identifying pool contains examples that more strongly pin down a unique rule. Importantly, the *test set* (query distribution) is kept the same across the two conditions; only the demonstration pool differs.

Prompt template. Given a demonstration set $\{(x_j, y_j)\}_{j=1}^k$, we format the prompt as

Question: $(x_1, ?, y_1), \dots, (x_k, ?, y_k). \quad x_{\text{test}}, ?,$

and instruct the model to output a single answer token span in English (sport name for Sports; person name for People).

Evaluation. For each task and each condition (ambiguous / identifying), we generate 100 prompts per random seed by sampling $k \in \{2, 4, 8\}$ uniformly and sampling k demonstrations uniformly without replacement from the corresponding pool. The query pair $(x_{\text{test}}, y_{\text{test}})$ is sampled from a fixed test list with ground-truth labels. Model outputs are parsed into JSON and normalized by lowercasing and removing punctuation; accuracy is computed by exact match with the normalized ground truth. We repeat the entire procedure for 5 random seeds and report mean \pm standard deviation across seeds.

Results. Tables 2–3 summarize the accuracy under the two demonstration pools as a function of k on Qwen-235B-A22B and Qwen-30B-A3B, respectively. Across both tasks, the identifying pool consistently yields higher accuracy than the ambiguous pool, and the performance gap generally increases with more demonstrations.

Table 2: **Demonstration Experiment.** Task: sports, repeated 5 times with different random seeds.

Demo number	Ambiguous Acc (235B)	Identifying Acc (235B)	Ambiguous Acc (30B)	Identifying Acc (30B)
2	0.265 \pm 0.073	0.421 \pm 0.080	0.122 \pm 0.029	0.176 \pm 0.062
4	0.267 \pm 0.084	0.542 \pm 0.048	0.151 \pm 0.078	0.410 \pm 0.059
8	0.202 \pm 0.037	0.602 \pm 0.043	0.164 \pm 0.039	0.559 \pm 0.074

Table 3: **Demonstration Experiment.** Task: People, repeated 5 times with different random seeds.

Demo number	Ambiguous Acc (235B)	Identifying Acc (235B)	Ambiguous Acc (30B)	Identifying Acc (30B)
2	0.713 \pm 0.074	0.940 \pm 0.049	0.735 \pm 0.083	0.908 \pm 0.059
4	0.708 \pm 0.096	0.931 \pm 0.027	0.775 \pm 0.037	0.950 \pm 0.058
8	0.648 \pm 0.008	0.845 \pm 0.044	0.820 \pm 0.027	0.990 \pm 0.001

H.3 Prompt Sensitivity vs. Demonstration Count

We study how token-level numerical predictions respond to changes in the in-context operator pattern while keeping the underlying query answer fixed. We evaluate Qwen3-30B-A3B model and Qwen3-235B-A22B model.

Prompt regimes. Each evaluation prompt consists of a fixed-format arithmetic query paired with a fixed target answer (e.g., 1345). We construct three regimes that differ only in the operator pattern appearing in the demonstrations: (i) *addition-only*, where all in-context examples use +; (ii) *multiplication-only*, where all examples use \times ; and (iii) *mixed-symbol*, where different operators are interleaved across demonstrations. Across all regimes, the query problem and its correct final answer remain identical.

Token-level score extraction. For each prompt, we extract token-level scores corresponding to the correct digits of the target answer. Concretely, for a target digit string $a_1a_2 \cdots a_L$, we record, at each output position ℓ , the model-assigned log-probability of the correct digit a_ℓ . These per-digit log-probabilities serve as a fine-grained proxy for the model’s confidence in the correct numerical prediction at each position. Specifically, in the figures, Char 1, 3, 4, 5 denotes the score trace associated with the 1, 2, 3, 4-th digit position of the fixed target answer 1345.

Findings. Figure 3 and Figure 4 present the token-level score trajectories for the Qwen3-235B-A22B and Qwen3-30B-A3B models, respectively, under the three operator regimes. Corresponding score gradients are shown in Figure 5 and Figure 6. In homogeneous-symbol regimes (addition-only or multiplication-only), per-digit score trajectories are relatively smooth and exhibit small discrete gradients, indicating stable symbolic behavior. In contrast, the mixed-symbol regime produces larger variance and more frequent sign changes in the gradients, suggesting increased instability when the operator distribution shifts within the context. These patterns are consistent across model scales, although the larger Qwen3-235B-A22B model exhibits systematically smaller gradient magnitudes, indicating improved robustness to symbolic heterogeneity.

H.4 CoT Effect

We further study the impact of CoT prompting on Llama3.2-3B, focusing on how the intermediate steps of the reasoning chain affects performance. We consider two CoT variants for the same multi-digit addition problem, which lead to the same correct final answer but differ in how intermediate steps are constructed.

In-distribution decomposition CoT. For the *in-distribution decomposition* CoT variant, each intermediate reasoning step corresponds to a well-defined subtask (e.g., digit-wise decomposition and carry propagation). To ensure that the model has intrinsic capability for these intermediate

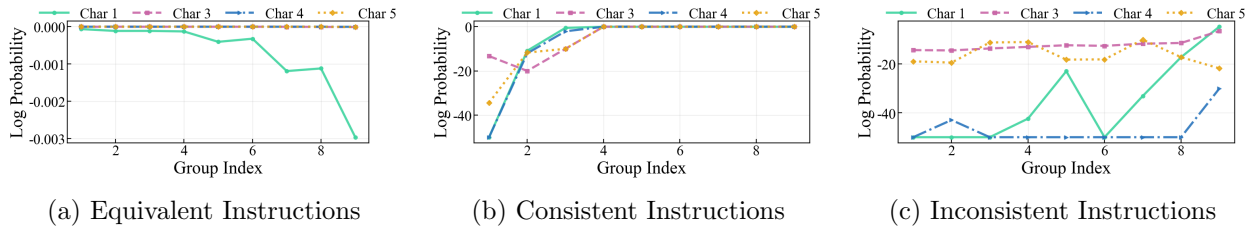


Figure 3: **Posterior confidence under instruction variation.** (Qwen-235B-A22B-Instruct) (a) Equivalent instructions yield stable, high-confidence predictions. (b) Incorrect but consistent instructions allow confidence to recover as more demonstrations are added. (c) Incorrect and inconsistent instructions lead to persistently low and unstable confidence despite increasing context length.

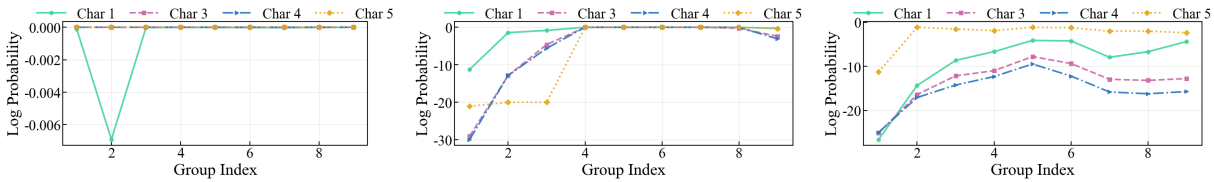


Figure 4: **Posterior confidence under instruction variation.** (Qwen-30B-A3B-Instruct) (a) Equivalent instructions yield stable, high-confidence predictions. (b) Incorrect but consistent instructions allow confidence to recover as more demonstrations are added. (c) Incorrect and inconsistent instructions lead to persistently low and unstable confidence despite increasing context length.

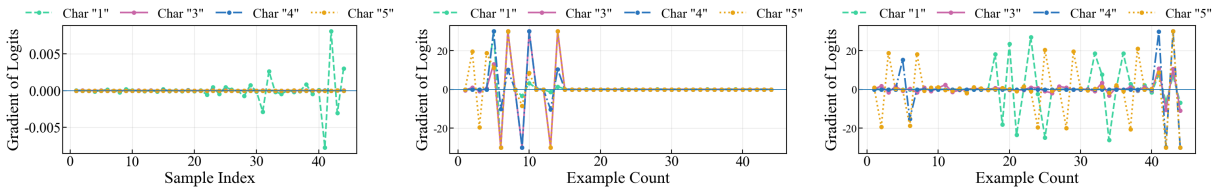


Figure 5: **Discrete gradients of log probability.** (Qwen-235B-A22B-Instruct) (a) Equivalent instructions yield small and stable gradients. (b) Incorrect but consistent instructions show gradual stabilization. (c) Incorrect and inconsistent instructions produce large and irregular gradients.

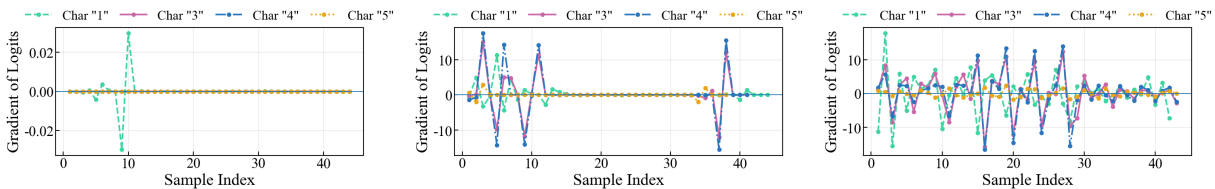


Figure 6: **Discrete gradients of log probability.** (Qwen-30B-A3B-Instruct) (a) Equivalent instructions yield small and stable gradients. (b) Incorrect but consistent instructions show gradual stabilization. (c) Incorrect and inconsistent instructions produce large and irregular gradients.

steps, we generate 10,000 training examples for *each* step and fine-tune the model on these step-level datasets prior to evaluation. Each example is formatted as an instruction–input–output triple, analogous to the pretraining setup in Section H.1.

- Step 1:** $1234561 = 1234560 + 1$
- Step 2:** $1323212 = 1323210 + 2$
- Step 3:** $1234560 + 1323210 \rightarrow (123456 + 132321) \times 10$
- Step 4:** $1 + 2$
- Step 5:** Combine results.

Each step corresponds to a sub-computation the model can reliably perform in isolation.

Out-of-distribution decomposition CoT. For the *out-of-distribution* CoT variant, the final answer remains correct, but the intermediate steps are constructed in a form that the model has *not* been explicitly trained on. In this case, no additional fine-tuning is performed for the intermediate steps, and the model is required to follow the reasoning chain purely through prompting.

- Step 1:** $1234561 = 1000000 + 234561$
- Step 2:** $1323212 = 1000000 + 323212$
- Step 3:** Add corresponding components. $1000000+1000000 = 2000000, 234561+323212 = 557773$
- Step 4:** Combine results.

Although logically correct, these intermediate steps do not correspond to well-supported arithmetic routines in the model’s pretraining distribution and provide little useful guidance for subsequent inference.

Training Setup. All fine-tuning for the good CoT variant uses the same LoRA configuration, optimizer, and training hyperparameters as in Section H.1. In particular, the architecture, learning rate, number of epochs, batch size, and quantization settings are kept fixed. This isolates the effect of step-level intrinsic capability from other confounding factors.

Results. We find that the grounded chain substantially improves accuracy over direct prompting without CoT, whereas the ungrounded chain provides no benefit and can even degrade performance (Figure 1b). This indicates that CoT prompting is effective only when each reasoning step is well-learned in pretrained sub-tasks, supporting our view of CoT as a sequence of structured in-context updates rather than an arbitrary logical derivation.